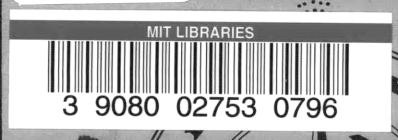

#1

DEPARTMENT OF THE NAVY

HYDROMECHANICS

AERODYNAMICS

STRUCTURAL MECHANICS

APPLIED MATHEMATICS

ACOUSTICS AND VIBRATION

PROGRESS IN AIR CUSHION VEHICLES

by

Allen G. Ford

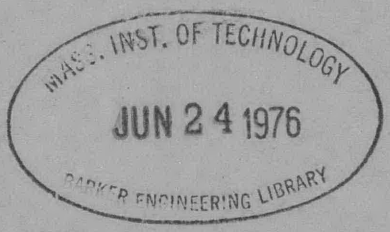

AERODYNAMICS LABORATORY

RESEARCH AND DEVELOPMENT REPORT

October 1966 Report 2280

PRNC-TMB-648 (Rev 1-64)

PROGRESS IN AIR CUSHION VEHICLES

by

Allen G. Ford

October 1966

Report 2280
Aero Report 1116

Foreword

This report is based on a paper given at the Ninth Navy Science Symposium in Washington, D. C., on May 5-6, 1966, sponsored by the Office of Naval Research. The paper incorporates much of the material on power predictive methods contained in a lecture series delivered by the author and Dr. Harvey R. Chaplin at the von Karman Institute in Brussels, Belgium, in May 1965, and published subsequently as a David Taylor Model Basin Report series.

NOTATION

b	beam of pressure region (or bubble), feet
C	cushion perimeter, feet
C_{D_e}	external aerodynamic drag coefficient $\left(\frac{D_e}{q_a S}\right)$
C_{D_o}	total drag coefficient for those quantities involving q_a and q_o (i.e., varying with V^2) $\left(\frac{D_o}{q_a S}\right)$
C_{D_t}	trunk drag coefficient $\left(\frac{D_t}{q_a S}\right)$
C_f	skin friction coefficient
C_L	lift coefficient $\left(\frac{L}{q_a S}\right)$
C_c, D_c	discharge coefficient $\left(Q \div (S_g V_c)\right)$
D_e	external aerodynamic drag, pounds
D_o	total drag when q_a and q_o apply, pounds
D_r	ram or momentum drag, pounds
$D_{s,a}$	additional sideboard (or sidewall) drag, pounds
$D_{s,w}$	secondary wavemaking drag associated with the drag of that amount of sideboard required to retain the bubble (or cushion), pounds
D_t	trunk drag, pounds
D_w	wavemaking drag, pounds
F_ℓ	length Froude number, $V/\sqrt{g\ell}$ (nondimensional)
$f_{\ell,}$	abbreviation for ordinate values of Figure 4
G	skirt or trunk drag geometry factor (nondimensional)

NOTATION (Continued)

H	average wave height, trough to crest, feet
h	daylight clearance; the height of ACV above a hard surface, feet
h_a	depth of fully wetted additional sideboard, feet
h_b	height difference between bottoms of fore and aft ski, feet
$K_{c,i}$	ideal cushion power parameter $\left(\frac{\beta}{c} \div \Delta p/p_t\right)$
L	lift of ACV, pounds
ℓ, ℓ_B	length of pressure region (or bubble), feet
ℓ_s	sideboard wetted length, feet
ℓ'	shortened wetted length of ACV with daylight clearance
$\dot{m}$	mass flow rate, slugs/sec
n	number of sideboard wetted sides; n = 4 for 2 sideboards
p, Δp	pressure (gage), lb/ft^2
$P_{c,i}$	ideal cushion power, lb-ft/sec
P_i	total ideal power, lb-ft/sec
$P_{p,i}$	ideal propulsion power, lb-ft/sec
p_t	total pressure at nozzle exit (gage), lb/ft^2
Q	flow quantity rate, ft^3/sec
q_a	dynamic air pressure $\left(\frac{1}{2} \rho_a V^2\right)$, lb/ft^2
q_w	dynamic pressure of water $\left(\frac{1}{2} \rho_w V^2\right)$, lb/ft^2
S	cushion base area, ft^2
S_g	daylight gap area (cushion perimeter times mean daylight gap, h), ft^2
S_p	propeller area, ft^2

NOTATION (Concluded)

V	velocity, ft/sec
V_c, V_j	cushion-reference velocity $\sqrt{\frac{2}{\rho}\Delta p}$; or jet velocity of air discharge from ACV base, when fully contracted, ft/sec
V_k	forward velocity, knots
V_o	forward velocity, ft/sec
$W = L$	air cushion vehicle (ACV) weight (or lift), pounds
w	ACV specific weight (W/S), lb/ft^2
α	vehicle pitch angle or angle of attack
ρ, ρ_a	air density, $slugs/ft^3$
ρ_w	water density, $slugs/ft^3$
η	propulsive efficiency
$\propto$	symbol for "is proportional to"

TABLE OF CONTENTS

LIST OF ILLUSTRATIONS

TABLE OF CONTENTS (Concluded)

LIST OF ILLUSTRATIONS (Concluded)

SUMMARY

An analysis is made of the various drag and power components applicable to the Captured Air Bubble (CAB) vehicle and to Hovercraft. These are wavemaking drag, sideboard drag, skirt (or trunk) drag, external aerodynamic drag, ram (or momentum) drag, and cushion power. Equations for the components are used to follow the main trends in Hovercraft and CAB development, wave drag playing an important role in the latter case. However, it is found that the equations for the two craft show no fundamental differences of kind, only differences of degree.

The subject of propulsor efficiency is then treated for the air propeller. It is shown that to achieve high efficiencies, large propeller-area/base-area ratios are required. Water propulsor systems are then suggested as a means of obviating the disc-area problem, although significant development would be required in this case.

Finally, a comparison of vehicles is made on the basis of weight/power ratio. The indicated performance potential of air cushion vehicles (ACV's), of both the Hovercraft and the CAB types, is shown to be very high compared with other vehicles in high-speed over-water operation.

INTRODUCTION

Vehicles operating over water fall into various classes, based upon their principal means of support when at their normal operating speed (Figure 1). (At rest or low speeds, of course, all depend upon hydrostatic forces.) The first class of vehicle is the displacement hull, which is supported by direct hydrostatic forces. The planing hull and the hydrofoil, on the other hand, are supported principally by hydrodynamic forces when at speed. A third class, represented by craft such as the ram wing and the wing-in-ground-effect, depends upon aerodynamic lift. The vehicles of the fourth category, which is the topic of this report, are known generally as air cushion vehicles (ACV's), and receive their support from aerostatic forces. Vehicles

of this category have various configurations and are classified roughly as follows:

1. The full-peripheral Air Cushion Vehicle (ACV) or full-peripheral Ground Effect Machine (GEM) or the Hovercraft or Hydroskimmer. These vehicles exist with or without flexible skirts (trunks).

2. The Air Lubricated Hull, or Hydrokeel.

3. The Captured Air Bubble (CAB), or sidewall ACV, or sidewall GEM with compliant or flexible end seals (or skirts or trunks at low "daylight" clearance). A second type (not shown) is a sidewall ACV with no flexible end seals (only an air curtain below the hard structure).

An experimental research vehicle, the CAB XR-1 is shown (Figure 2) in smooth water at a speed of approximately 30 knots (Froude number $F_\ell = 1.5$). The XR-1 is a 10-ton Navy experimental research craft with a bubble length/beam ratio of 3.5 (see Reference 1). Because of stability problems with the vehicle, it is presently undergoing modifications, which include a 50-percent beam increase.

The British Westland 10-ton SRN-6, shown in Figure 3 is a stretched version of the SRN-5, a seven-ton Hovercraft. The U. S. Navy has purchased three of the latter craft from Bell Aerosystems Company, Westland's U. S. licensee, for duty in Viet Nam.

This report is concerned chiefly with the drag and power of the aerostatic ACV with some emphasis on the CAB, which has been an in-house Navy development effort at the Naval Air Development Center, Johnsville, Pennsylvania, the Naval Air Engineering Center, Philadelphia, Pennsylvania, and the David Taylor Model Basin, Washington, D. C. Also receiving special consideration is the British Hovercraft, as representative of the full-peripheral ACV. This report incorporates much of the material of References 2 through 5.

DRAG

A comprehensive analysis of the various drag components applicable to aerostatic vehicles, especially the CAB and full-peripheral ACV will be given. After each topic is considered separately, a simplified summary will be possible.

WAVEMAKING DRAG

A region of pressure, proceeding at some speed V over a body of otherwise calm water, generates waves. If the pressurized region is considered to be at rest, and the otherwise calm water has a velocity of -V, then the wave pattern generated is fixed in space.

Our interest in this wave is that an ACV pressure region generates such a wave, and further that the pressure region ultimately acts back on the vehicle to give a resultant air pressure force tilting back somewhat from the vertical. This tilted force has, in addition to a lift component, a drag component, which will be called a wavemaking drag, D_w .

The wavemaking problem of a constant pressure region of finite dimensions is a difficult one. Fortunately this work has been accomplished in recent years at the David Taylor Model Basin (Reference 6). Figure 4 shows these results for a rectangular distribution of constant pressure. The wave drag parameter f_ℓ plotted on the ordinate (drag/lift ratio divided by pressure/length ratio and constants) is plotted against the length Froude number $V/\sqrt{g\ell}$. It can be noted that the wave drag D_w is proportional to lift L, to pressure p, the wave drag parameter f_ℓ , and is reciprocally proportional to pressure (or bubble) length ℓ_B . The value of the wave drag parameter f_ℓ depends only on the length/beam (ℓ/b) ratio and Froude number F_ℓ . The speeds of maximum f_ℓ are referred to as "hump speeds" or "hump Froude numbers." In the sub-hump region, the slopes of the lines in Figure 4 were adjusted to the slopes of early British Hovercraft experimental data (Reference 7). The actual below-hump speed shape of f_ℓ is probably different from that shown in Figure 4. The simplification mentioned above is justified only because the below-hump-speed values are relatively unimportant to the task at hand. Secondary drag humps and valleys can exist, however, and they could be of considerable significance for some purposes.

The resultant ratio of wave drag to lift (or drag/weight) is written, based on Figure 4. The pressure p can be replaced by specific weight w if the entire load is on the bubble rather than partially on the seals. For the purpose of specifying wave drag, this conservative assumption will be made. Later, however, a seal (or trunk) drag penalty will also be derived.

$$\frac{D_w}{W} = \frac{4p}{\rho_w g \ell} \cdot f_\ell \qquad [1]$$

If external aerodynamic lift $\left(C_L\ q_a\ S\right)$ provides partial vehicle support, then the cushion pressure is less than the vehicle specific weight w, which is W/S. In terms of the vehicle specific weight w, the wave drag/weight ratio is

$$\frac{D_w}{W} = \frac{4}{\rho_w g}\ \frac{w}{\ell_B}\ \left(1 - \frac{C_L\ q_a}{w}\right)^2 f_\ell \qquad [2]$$

SIDEWALL DRAG IN A CAPTURED AIR BUBBLE TYPE OF AIR CUSHION VEHICLE

A sketch of a CAB ACV in an above-hump speed condition is shown in Figure 5. The angle α is exaggerated to point out two regions of sidewall wetting and drag.

A primary function of sidewalls (or sideboards or side skegs) is to prevent loss of air along the side of the vehicle. This is done by a triangularly wetted sideboard section of maximum wetted height h_b; that is, wetted on the outside only. This wetted area is referred to as sidewall due to the bubble. The assumption here is that the outside water line continues horizontally; whereas, the inside water line is turned down by the angle α.

Below this triangular region of sideboard due to the bubble is a region referred to as "additional sidewall," which is fully wetted, both inside and outside.

ADDITIONAL SIDEWALL DRAG — The amount of additional sidewall depth h_a (Figure 5) in smooth water would be held to a minimum at high speeds, but would be increased for transiting the hump speed. In waves at high speed, fore and aft seals or skis (skirts or trunks at zero "daylight" clearance) are set very close to the bottom of the sidewalls, but waves of height H will nevertheless wet an equivalent height h_a of approximately one-half the average wave height.

$$h_a = \frac{1}{2} H \qquad [3]$$

The reason for this is that (for the above ski setting) the bottom of the sidewall runs at the wave trough, and the fore and aft skis or seals move up and down rapidly, staying very close to the water surface.

The additional sidewall drag is given by the product of the skin friction coefficient C_f , the dynamic pressure in water q_w , and the wetted area. Wetted area is the product of sidewall length ℓ_s , wetted height h_a , and number of wetted sides n . The additional sidewall drag/weight ratio is then, for n equal 4:

(Same as sidehull fric drag)

$$\frac{D_{s,a}}{W} = \frac{C_f \, q_w \, n \, \ell_s \, h_a}{\ell_B \, w \, b} \qquad [4]$$

$$\frac{D_{s,a}}{W} = 4 \, \frac{\ell_B}{b} \frac{\ell_s}{\ell_B} \, C_f \, \frac{q_w}{w} \frac{h_a}{\ell_B} \qquad [5]$$

sidehull wave

SECONDARY WAVEMAKING DRAG OR SIDEWALL DRAG DUE TO RETAINING THE AIR BUBBLE — Figure 5 shows triangularly wetted sidewall sections of maximum wetted height h_b that are wetted on the outside only. These triangular sections prevent air loss along the vehicle sides. Their total water wetted area for the whole vehicle is $h_b \, \ell_B$. The drag is the product of the drag coefficient C_f , water dynamic pressure q_w , and wetted area $\ell_B \, h_b$.

$$\frac{D_{s,w}}{W} = \frac{C_f \, q_w \, \ell_B \, h_b}{\ell_B \, w \, b} = \frac{\ell_B}{b} \, C_f \, \frac{q_w}{w} \frac{h_b}{\ell_B} \qquad [6]$$

From Figure 5, it can be seen that

$$\frac{h_b}{\ell_B} = \frac{D_w}{W} \qquad [7]$$

Thus,

$$\frac{D_{s,w}}{W} = \frac{\ell_B}{b} \, C_f \, \frac{q_w}{w} \frac{D_w}{W} \qquad [8]$$

The expression [8] is for a CAB type of ACV with sidewalls, and no appreciable daylight clearance h.

Figure 6 shows a sidewall ACV with some daylight clearance h, but with the sidewall still wetted to some extent on the outside. The wetted height is $(h_b - h)$; the wetted length is ℓ', and

$$\ell' = \frac{h_b - h}{h_b/\ell_B} = \frac{\left(\frac{D_w}{W}\ell_B - h\right)}{\frac{D_w}{W}} \qquad [9]$$

The wetted area is the product of ℓ' and $(h_b - h)$.

$$\text{Wetted Area} = \frac{\left(\frac{D_w}{W}\ell_B - h\right)^2}{\frac{D_w}{W}} = \frac{\ell_B^2\left(\frac{D_w}{W} - \frac{h}{\ell_B}\right)^2}{\frac{D_w}{W}} \qquad [10]$$

In this case

$$\frac{D_{s,w}}{W} = \frac{C_f\, q_w}{\ell_B\, w\, b} \cdot \frac{\ell_B^2\left(\frac{D_w}{W} - \frac{h}{\ell_B}\right)^2}{\frac{D_w}{W}} \qquad [11]$$

Or

$$\left.\begin{aligned} \frac{D_{s,w}}{W} &= \frac{\ell_B}{b} C_f \frac{q_w}{w} \cdot \frac{\left(\frac{D_w}{W} - \frac{h}{\ell_B}\right)^2}{\frac{D_w}{W}} \quad , \quad \frac{D_w}{W} - \frac{h}{\ell_B} \geq 0 \\ &= 0 \quad , \quad \frac{D_w}{W} - \frac{h}{\ell_B} < 0 \end{aligned}\right\} \qquad [12]$$

This equation is valid for a more general case than [8]. It is valid for a sidewall ACV with some daylight clearance h; but, nevertheless, with some wetted area, as shown in Figure 6. When h/ℓ_B equals and then exceeds D_w/W, this drag becomes and remains zero.

In spite of the complexity of [12], the expression can be shown to be nearly constant and hence does not affect optimizations. Moreover, the term is small in all cases.

For the usual Hovercraft case it would satisfy the condition for being zero (or nearly zero) in [12]. In the CAB case, substituting [1] into [8] yields a conservative statement of $\overbrace{D_{s,w}}$ (ignores external aerodynamic lift and thus overestimates $D_{s,w}$) as follows:

$$\frac{D_{s,w}}{W} = \frac{\ell_B}{b} C_f \frac{q_w}{w} \left[\frac{4}{\rho_w g} \frac{w}{\ell_B} f_\ell \right] \qquad [13]$$

It can be deduced from Figure 4 that f_ℓ is approximately proportional to F_ℓ^{-2} for low ℓ/b values, and that a reasonable fit to f_ℓ is given by $0.5/F_\ell^2$ (for speeds above hump speed). This line intersects the $(\ell/b = 2)$ line at $(F_\ell = 2)$, and has a slope of minus two.

Relating Froude number F_ℓ to q_w/w:

$$F_\ell = \frac{V}{\sqrt{g\ell_B}} = \left(\frac{2}{\rho_w g} \right)^{\frac{1}{2}} \left(\frac{w}{\ell_B} \right)^{\frac{1}{2}} \left(\frac{q_w}{w} \right)^{\frac{1}{2}} \qquad [14]$$

Substituting these relationships into [13] yields a very simple form as follows:

$$\frac{D_{s,w}}{W} \approx \frac{4}{\rho_w g} C_f \frac{w}{\ell_B} \frac{\ell_B}{b} \frac{q_w}{w} \left[0.5 \frac{\rho_w g}{2} \frac{\ell_B}{w} \frac{w}{q_w} \right] \qquad [15]$$

$$\frac{D_{s,w}}{W} \approx C_f \frac{\ell_B}{b} \qquad [16]$$

SIDEWALL WAVEMAKING DRAG AND FORM DRAG — Because of the high fineness ratios of CAB type ACV sidewalls, and low immersed depths when "on the bubble," sidewall wavemaking drag is usually negligible (Reference 8). Form drag of water-immersed portions is also usually

negligible because of the high fineness ratios and low immersions (Reference 9). The profile drag, made up of skin friction and pressure form drag, is then closely equal to the skin friction drag.

TRUNK OR SKIRT DRAG IN FULL-PERIPHERAL AIR CUSHION VEHICLES

The most important new element which the British have introduced in air cushion vehicle technology is flexible trunks, or skirts, as illustrated in Figure 1. These trunks have in no way changed the basic principles of air cushion vehicles, but they have had a very profound effect on the design choices that the designer is likely to make. The most obvious effect on the designer's choice is in the question of the "daylight" gap (the clearance between the bottom of the skirt and the water) and in the hard structure clearance (clearance between the hard structure of the vehicle and the water). The introduction of trunks has caused the designer to choose much lower values of the daylight gap and much higher values of the hard structure clearance. These choices involve design tradeoffs; for example, the choice of daylight gap clearance involves the tradeoff between lift power and propulsion power. Using small values of daylight clearance, the lift power is greatly reduced. On the other hand, as soon as the vehicle operates not on a smooth surface, but in a seaway, the flexible trunk drags through the water and there is an increase in propulsive power required.

The only definitive information readily available on the subject of the drag associated with pulling flexible trunks through waves is represented in Figure 7. It comes from the tests of the VA-3 Hovercraft conducted by Republic Aviation under contract to the Office of Naval Research (Reference 10).

In the left graph of Figure 7, a trunk drag coefficient, referred to cushion area and the dynamic pressure of air, is plotted versus the ratio of wave height to cushion length for two different values of daylight clearance. It was then surmised that air cushion vehicles tend to average out the waves over which they fly, and therefore significant trunk drag should not occur until the wave height exceeds twice the daylight clearance. On this basis, in the right graph in Figure 7, the same

data were replotted versus the ratio of the wave height, less twice the daylight clearance, to cushion length. It was found that the data then fell nearly on a single line, which could be represented by a very simple nondimensional formula. This formula is an empirical expression of the VA-3 trunk drag. It is not known whether the drag characteristics of the VA-3 trunks are favorable or unfavorable compared with other designs. Since, however, these are the only definitive data available, this formula will be applied directly to estimate performance in a sea state.

The trunk drag coefficient C_{D_t} is a function of the average wave height H, the ACV length ℓ, and the daylight clearance h. The drag coefficient C_{D_t} is the drag per unit cushion area S, and per unit air dynamic pressure q_a .

$$C_{D_t} = 6.6 \left(\frac{H - 2h}{\ell}\right)^{1.2} \qquad [17]$$

The trunk drag/weight ratio is then,

$$\left.\begin{aligned} \frac{D_t}{W} &= \frac{C_{D_t} S\, q_a}{\ell_B\, w\, b} = \frac{C_{D_t}\, q_a}{w} \\ &= 0.0012\, \frac{C_{D_t}\, q_w}{w} \end{aligned}\right\} \qquad [18]$$

$\frac{\rho_a}{\rho_w} = \frac{1}{64}$.

Thus,

$$\left.\begin{aligned} \frac{D_t}{W} &= 6.6\, \frac{q_a}{w} \left(\frac{H - 2h}{\ell}\right)^{1.2} \\ &= 0.00792\, \frac{q_w}{w} \left(\frac{H - 2h}{\ell}\right)^{1.2} \end{aligned}\right\},\quad (H - 2h) \geq 0$$

$$= 0 \qquad ,\quad (H - 2h) < 0 \qquad [19]$$

CAPTURED AIR BUBBLE AIR CUSHION VEHICLE SEAL OR SKI DRAG

The fore and aft seals or skis on CAB ACV's (and models) have been of a mechanical type principally, but the advantages of low-weight fabric materials, relative to high-frequency response, are evident. For this reason an analogy can be drawn to full-peripheral ACV trunks; and Equation [19], times a geometric factor G, can be used tentatively for CAB type ACV seal or ski drag. This geometry factor, G, is less than 1, and depends on the length-to-beam ratio of a CAB ACV. It is tentatively given as the reciprocal of $(1 + \ell/b)$. If we put G into Equation [19], it takes a value of 1 for the full-peripheral ACV.

EXTERNAL AERODYNAMIC DRAG

The external aerodynamic drag is given by the product of the drag coefficient C_{D_e}, the reference base cushion area S, and the air dynamic pressure q_a. The external aerodynamic drag/weight ratio is then,

$$\frac{D_e}{W} = \frac{C_{D_e} S q_a}{\ell_B w b} = \frac{C_{D_e} q_a}{w} \qquad [20]$$

RAM OR MOMENTUM DRAG

The ram or momentum drag arises from bringing a constant mass flow rate of air $\dot{m}$ from a velocity V relative to the ACV to a zero velocity relative to the ACV. Thus,

$$D_r = \dot{m} V = \rho V_j \left(D_c S_g \right) V_o \qquad [21]$$

where ρV_j is the mass flow rate per unit area near the ACV base (where the flow is fully contracted), V_o is the vehicle velocity, and $D_c S_g$ is the fully contracted flow area. The daylight gap (clearance) area is S_g, and D_c is the discharge coefficient.

The weight W equals wS, and the ram drag/weight ratio is given by

$$\frac{D_r}{W} = \frac{\left(2\ \rho_a\right)^{\frac{1}{2}} \left(\frac{1}{2}\ \rho_a\ V_j^2\right)^{\frac{1}{2}} \mathscr{C}_c\ S_g \left(\frac{2}{\rho_a}\right)^{\frac{1}{2}} \left(\frac{1}{2}\ \rho_a\ V_o^2\right)^{\frac{1}{2}}}{wS} \qquad [22]$$

$$= \frac{2\ p^{\frac{1}{2}} \left(\mathscr{C}_c\ S_g\right) q_a^{\frac{1}{2}}}{wS} \qquad [23]$$

$$= \frac{2\ w^{\frac{1}{2}} \left(1 - C_L \frac{q_a}{w}\right)^{\frac{1}{2}} D_c\ S_g\ q_a^{\frac{1}{2}}}{wS} \qquad [24]$$

$$\frac{D_r}{W} = 2\ D_c \left(1 - C_L \frac{q_a}{w}\right)^{\frac{1}{2}} \left(\frac{q_a}{w}\right)^{\frac{1}{2}} \frac{S_g}{S} \qquad [25]$$

DRAG SUMMARY

The total drag/lift (drag/weight) ratio D_T/W is given as an appropriate summation of the previously derived component drag/lift ratios. These component ratios are repeated here for convenience.

$$\frac{D_w}{W} = \frac{4}{\rho_w g} \frac{w}{\ell_B} \left(1 - \frac{C_L\ q_a}{w}\right)^2 f_\ell \qquad [2]$$

$$\left.\begin{aligned} \frac{D_{s,w}}{W} &\approx \frac{\ell_B}{b} C_f \quad , \quad \frac{h}{\ell_B} \ll \frac{D_w}{W} \\ &= 0 \quad , \quad \frac{h}{\ell_B} \geq \frac{D_w}{W} \end{aligned}\right\} \qquad [16]$$

$$\frac{D_r}{W} = 2 D_c \left(1 - C_L \frac{q_a}{w}\right)^{\frac{1}{2}} \left(\frac{q_a}{w}\right)^{\frac{1}{2}} \frac{S_g}{S} \qquad [25]$$

Equations [5], [19], and [20] can be condensed by grouping as follows:

$$\frac{D_o}{W} = C_{D_o} \frac{q_w}{w} \qquad [26]$$

where the total drag coefficient C_{D_o} is

$$C_{D_o} = \left[2\left(\frac{\ell_s}{\ell_B}\right) C_f \left(\frac{\ell_B}{b}\right) \frac{H}{\ell_B} + 0.00792 \left(\frac{H - 2h}{\ell}\right)^{1.2} G + 0.0012 C_{D_e} \right] \qquad [27]$$

where G = 1 for full-peripheral ACV's, and G = $\left(\frac{1}{1 + \ell/b}\right)$ for CAB ACV's. Any summation to obtain a total drag/lift ratio D_T/W should then consider these questions.

POWER

Thus far the subject of "Drag" has been covered. The real interest in the subject of drag follows from the investment of power to overcome it in providing vehicle thrust. A second source of power expenditure in ACV's; namely, cushion fan power, is now discussed. After this, the topics of total ideal specific power and propulsor efficiency are treated.

CUSHION POWER

The cushion fan power must necessarily be explained in terms of the type of vehicle — simple plenum or peripheral-jet ACV.

PLENUM — The simple plenum craft of Figure 8 is comparatively easy to understand, yet possesses most of the characteristics of aerostatic ACV's or Ground Effect Machines (GEM's) that must be

understood, if one is to understand GEM's at all. The cushion is contained in a large cavity, between the ground, the base of the craft, and the "plenum walls" extending down from the base. Air is pumped directly into the cushion through a compressor, and escapes through a "daylight gap" at the lower edge of the cushion, at velocity V_c. If we choose the primary variables to be:

Cushion Area	S	ft^2
Cushion Perimeter	C	ft
Daylight Gap	h	ft
Cushion Pressure	Δp	psfg
Discharge Coefficient	D_c	---

then other properties of the system follow directly:

Lift = Weight	$W = wS \doteq \Delta p\ S$	lb
Gap Area	$S_g = h\ C$	ft^2
Reference Velocity	$V_c = \sqrt{\frac{2}{\rho_a}\Delta p}$	ft/sec
Flow Quantity	$Q = V_c\ S_g\ D_c$	ft^3/sec
Ideal Cushion Power	$P_{c,i} = \Delta p\ Q$	lb-ft/sec

These relationships become slightly modified with forward speed, V_o, when the dynamic pressure $\left(q = \rho_a\ V_o^2/2\right)$ becomes comparable in magnitude to the cushion pressure Δp. At moderate speeds, however, we can write:

Cushion Specific Power (Ideal)

$$\frac{P_{c,i}}{W\ V_o} = \frac{\Delta p\ Q}{wS\ V_o} = \frac{S_g\ D_c\ V_c}{S\ V_o}\left(1 - C_L\frac{q_a}{w}\right)$$

$$= \frac{S_g}{S}\ D_c\ \frac{\sqrt{\frac{2\ \Delta p}{\rho}}}{\sqrt{\frac{2}{\rho}}\sqrt{\frac{1}{2}\ \rho\ V_o^2}}\left(1 - C_L\frac{q_a}{w}\right)$$

$$= \frac{S_g}{S}\ \frac{D_c}{\sqrt{\frac{q_a}{\Delta p}}}\left(1 - C_L\frac{q_a}{w}\right)$$

$$= \frac{S_g}{S}\ \frac{D_c}{\sqrt{\frac{q_a}{w}}}\left(1 - C_L\frac{q_a}{w}\right)^{\frac{3}{2}} \quad \begin{cases} \text{Plenum} \\ \frac{q_a}{w} << 1 \end{cases} \qquad [28]$$

Actually, the ideal cushion power should include the effect of ram recovery, that is,

$$P_{c,i} = Q(\Delta p - q_a) \qquad [29]$$

Calculating the ideal ram recovery specific power by itself,

$$\frac{P_{i(rr)}}{W\ V_o} = \frac{Q\ q_a}{W\ V_o} = \frac{D_c\ V_j\ S_g\ q_a}{W\ V_o}$$

$$= D_c\ \frac{S_g}{S}\frac{q_a}{w}\frac{V_j}{V_o} = D_c\ \frac{S_g}{S}\frac{q_a}{w}\sqrt{\frac{\Delta p}{q_a}}$$

$$= D_c\ \frac{S_g}{S}\left(\frac{q_a}{w}\right)^{\frac{1}{2}}\left(1 - C_L\frac{q_a}{w}\right)^{\frac{1}{2}} \qquad [30]$$

The expression for ideal ram recovery specific power given in Equation [30] is exactly one-half of that for ram drag specific power (or ram-drag/weight, D_r/w) in Equation [25]. If one subtracts Equation [30] from Equation [25], then one-half of the expression for Equation [25] is the net result. Doing this broadens the range of applicability of Equation [28].

Note, however, that this ram recovery subtracts from the power that would otherwise be used on the cushion fan shaft.

PERIPHERAL JET — The plenum ACV and the peripheral-jet ACV are contrasted in Figure 9. It is possible to reduce the discharge coefficient D_c very substantially by discharging the air from the compressor at the periphery of the cushion, instead of directly into the cushion. This reduction of discharge coefficient is accomplished however, at the expense of increasing the total pressure of the compressor output from Δp (psfg) to p_t (psfg), where $p_t > \Delta p$. The ideal cushion specific power for the peripheral (or annular) jet is given by:

$$\frac{P_{c,i}}{W\ V_o} = \frac{p_t\ Q}{wS\ V_o} = \frac{p_t\ S_g\ D_c\ V_c}{wS\ V_o}$$

$$= \frac{S_g}{S}\ \frac{\Delta p}{w}\ \frac{D_c}{\frac{\Delta p}{p_t}}\ \sqrt{\frac{\Delta p}{q_a}}$$

$$\frac{P_{c,i}}{W\ V_o} = \frac{S_g}{S}\ K_{c,i}\ \frac{1}{\sqrt{\frac{q_a}{w}}}\left(1 - C_L\frac{q_a}{w}\right)^{\frac{3}{2}} \qquad [31]$$

where $K_{c,i} = D_c \Big/ \frac{\Delta p}{p_t}$ is the Ideal Cushion Power Parameter. Equations [28] for the plenum and [31] for the peripheral jet are now of the same form. Equation [30] (and Equation [25] as well) with D_c replaced by $K_{c,i}$ also follows. The latter equations, being more general, can

therefore be used for both the plenum and the peripheral jet. For a practical design, $K_{c,i}$ is likely to be roughly the same for the peripheral jet as for the plenum (perhaps 20 percent less); therefore, we no longer need draw any sharp distinction between cushions of the plenum type and of the peripheral jet type. Thus, performance of the two types will be considered to be about equivalent and, in any case, constant.

This discussion of cushion power has considered vehicle weight balanced in equilibrium by base pressure reaction and by external aerodynamic lift. A third force, jet reaction, can be shown to be negligible for most purposes when $S_g/S \ll 1$, a condition which holds for most of the important current vehicles. (See Reference 3 for a more detailed discussion of this topic.)

TOTAL IDEAL SPECIFIC POWER

The total specific power (often called "equivalent lift/drag ratio") is one of the more important of the various nondimensional vehicle performance parameters. For a fixed fuel-weight/gross-weight ratio, the vehicle range depends linearly upon it.

The total ideal specific power (ideal implies omission of propulsive and fan efficiency) is the sum of the cushion and propulsive ideal specific powers.

$$\frac{P_i}{W\ V_o} = \frac{P_{c,i}}{W\ V_o} + \frac{P_{p,i}}{W\ V_o} \qquad [32]$$

At this point it will prove useful to repeat in summary form both the drag/weight (or drag ideal specific power) equations and the cushion specific power equations derived thus far.

$$\frac{D_w}{W} = \frac{4}{\rho_w g}\ \frac{w}{\ell_B}\ \left(1 - \frac{C_L\ q_a}{w}\right)^2 f_\ell \qquad [2]$$

$$\left.\begin{aligned} \frac{D_{s,w}}{W} &\approx \frac{\ell_B}{b} C_f \quad , \quad \frac{h}{\ell_B} \ll \frac{D_w}{W} \\ &= 0 \quad , \quad \frac{h}{\ell_B} \geq \frac{D_w}{W} \end{aligned}\right\} \qquad [16]$$

$$\frac{D_r}{W} - \frac{P_{i(rr)}}{W V_o} = K_{c,i}\left(\frac{S_g}{S}\right)\left(\frac{q_a}{w}\right)^{\frac{1}{2}}\left(1 - C_L \frac{q_a}{w}\right)^{\frac{1}{2}} \qquad [25]\text{-}[30]$$

$$\frac{D_o}{W} = C_{D_o} \frac{q_w}{w} \qquad [26]$$

$$\frac{P_{c,i}}{W V_o} = \frac{S_g}{S} K_{c,i} \frac{1}{\sqrt{\frac{q_a}{w}}}\left(1 - C_L \frac{q_a}{w}\right)^{\frac{3}{2}} \qquad [31]$$

The common nondimensional parameter that appears thus far in the equations derived is

$$\sqrt{\frac{q_a}{w}} \quad , \quad \text{or} \sqrt{\frac{q_w}{w}}$$

(Note that $q_a = \frac{1}{2} \rho_a V^2 \approx 0.0012\ q_w$.)

We can usefully define a ("nondimensional") speed parameter $V_k/\sqrt{w}$, where $V_k \approx 17.2 \sqrt{q_a}$ is velocity in knots, as follows:

$$\frac{V_k}{\sqrt{w}} = 17.2 \sqrt{\frac{q_a}{w}} \qquad [33]$$

HOVERCRAFT — Figure 10 shows a logarithmic plot of the ideal specific power for a full-peripheral ACV or Hovercraft as a function of

this speed parameter. In this figure, Equation [31] is plotted (negative first-power slope) for two values of the product of $K_{c,i}$ (ideal cushion power parameter) and S_g/S (gap area ratio). Equation [26] (positive second-power slope) is also plotted for two values of the total drag coefficient C_{D_o}. The summation of these cushion and propulsive specific powers, Equation [32], is plotted as a dashed curve.

Figure 10 shows the dominant influence of the gap area ratio S_g/S, and of the drag coefficient C_{D_o}. If we regard each of the dashed curves as representing a specific design, then the minima of these curves are "optimum" points, in the sense of providing a minimum specific power and hence a minimum fuel consumption during a given trip.

Comparing different "designs" on this basis, the following (approximate) trends can be traced on Figure 10:

$$\left(\frac{V_k}{\sqrt{\Delta w}}\right)_{opt} \propto \left(\frac{S_g}{S}\right)^{\frac{1}{3}} C_{D_o}^{-\frac{1}{3}} \qquad [34]$$

$$\left(\frac{P_i}{W V_o}\right)_{opt} \propto \left(\frac{S_g}{S}\right)^{\frac{2}{3}} C_{D_o}^{\frac{1}{3}} \qquad [35]$$

That is,

1. With air gap ratio S_g/S fixed, the optimum speed decreases with increasing drag coefficient, in proportion to $C_{D_o}^{-\frac{1}{3}}$; the minimum specific power increases as $C_{D_o}^{\frac{1}{3}}$.

2. With total drag coefficient C_{D_o} fixed, the optimum speed increases with increasing air gap ratio in proportion to $(S_g/S)^{\frac{1}{3}}$; the minimum specific power, however, increases in proportion to $(S_g/S)^{\frac{2}{3}}$.

These interpretations depend upon the assumptions that:

1. The wave drag is "moderate." That is, D_w/W in Equation [2] must be comparatively small. For reasonably small values of the ratio w/ℓ_B, specific-loading/length, this is true.

2. The ram drag (minus ram recovery) is "moderate." That is, Equation [25] minus Equation [30] must be comparatively small. For reasonably small values of the product $\frac{V_k}{\sqrt{w}} \frac{S_g}{S}$, this should be true.

It is very enlightening to trace, qualitatively, one of the main trends of Hovercraft development on a graph like that of Figure 10. This is done in Figure 11.

The SR.N1 was allowed to have a relatively high drag coefficient C_{D_1} for reasons of economical construction; and had an air gap area S_g judged just sufficient to avoid water contact under "normal" conditions. This resulted in a rather large air gap ratio $(S_g/S)_1$, because the SR.N1 was small.

The SR.N2 was more streamlined, giving originally a smaller drag coefficient C_{D_2}. In the original design, the air gap height ("daylight clearance") h was about the same as for SR.N1 but the air gap area ratio $(S_g/S)_2$ was smaller, because the SR.N2 was larger. (For a given planform shape and given daylight clearance h, the ratio S_g/S is inversely proportional to the linear dimension of the planform.)

However, before SR.N2 was put into service, Westland changed the design, introducing flexible trunks and reducing the air gap ratio substantially to $(S_g/S)_2'$. The daylight clearance was no longer large enough to avoid water contact under "normal" conditions, so the total drag coefficient under average expected wave conditions was increased substantially, to $C_{D_2'}$, on account of the additional hydrodynamic drag.

The SR.N4 (projected 150-ton channel ferry) might have, according to information given in the press, about the same daylight clearance h; but again, a substantial decrease in air gap area ratio, to $(S_g/S)_4$, because of the increased planform dimensions. The average total drag

coefficient might go either up or down, relative to SR.N2, depending on how the respective average operating wave conditions are defined. In the above qualitative graph, it has been assumed that $C_{D_4} = C_{D_2}$.

It should be stressed, again, that the above-mentioned graph is only qualitative, and undoubtedly contains discrepancies as to the detailed relationships between specific craft. The general trend, however, toward ever smaller gap area ratios S_g/S, ever smaller specific power, and ever smaller optimum nondimensional speeds, is correctly represented.

Also correctly represented is the sharp break in the trend of development which occurred with the introduction of flexible skirts or trunks. One should not think that flexible trunks caused this break in the trend; but rather, that they permitted it. There was a substantial gain in operating economy to be had by reducing the air gap area S_g, even at the expense of greatly increased contact with the surface, and drag, and decreased (nondimensional) speed. Flexible trunks made this decreased gap area feasible from the standpoint of structural integrity, structural weight, and motions (passenger comfort). (Decreasing the air gap also has other advantages, besides reduced specific power; in particular, reduced size and weight of machinery and ducting.)

Of course, specific power is not the only performance parameter which is important. There are three parameters which are of paramount importance: specific power, ratio of empty weight to gross weight, and speed (dimensional; in knots, for example). Every successful vehicle is the result of a favorable balance between these three parameters.

The unfavorable trend toward lower nondimensional speeds, as the specific power is favorably reduced, has tended to be offset by increased cushion pressure and specific loading so that the dimensional speed has not decreased. (Actually, a slight trend toward higher actual speeds with larger vehicles can be justified.)

In fact, if Figure 10 were universally valid, we would not have to worry very much about speed. We could accept almost any design change, within reason, which improved the specific power; and then win back the desired speed by increasing the specific loading or cushion pressure. (The structural problems generally tend to become more tractable also,

with an increase in cushion pressure.) However, among the various qualifications placed on Figure 10, was the requirement that the cushion pressure be "moderate." It is now necessary to clarify this requirement, which has to do with the wavemaking drag of Equation [2].

The wavemaking drag varies in proportion to a negative power of V_k, at speeds above "hump speed," and so, obviously, Figure 10 does not at all apply if the wavemaking drag is very significant, in the vicinity of the optimum speed. Moreover, for a given planform shape and size, the wavemaking drag D_w (in proportion to gross weight W) varies directly with the specific loading w:

$$\frac{D_w}{W} \propto w \qquad [36]$$

Therefore, when we say Figure 10 is restricted to "moderate" cushion pressures, we mean, specifically, that it is restricted to cushion pressure sufficiently moderate that the wavemaking drag (D_w in Equation [2]) plays only a minor role in the determination of the optimum performance point.

The Westland family of Hovercraft SR.N1 through SR.N4 discussed above (and also SR.N5 and SR.N6, which are reversions to smaller-sized vehicles) satisfy the condition of "moderate" cushion pressure reasonably well. However, it would seem that, projecting that line of development into the future, to larger and larger vehicles, the cushion pressures would become less and less "moderate"; and optimum performance would be determined less and less adequately by the simple cushion power versus propulsion power tradeoff represented in Figure 10.

Rather than attempt to follow the subtle changes likely to take place in that line of development, however, it will be simpler, for our present purpose, to turn to a different line of development, in which we already find the cushion power playing a minor role, while the wavemaking drag plays a very major role.

CAPTURED AIR BUBBLE (CAB) -- Many of the early ideas and inventions of Ground Effect Machines included the idea of minimizing the air gap by use of slender sidewalls, extending into the water to block the escape of air from the cushion.

In the intensive early exploration of GEM's (from 1957 to 1961, say) the sidewall GEM received its due share of attention; but most investigators quickly concluded (perhaps prematurely) that, because of the hydrodynamic drag of the sidewalls, these craft would be suitable only for relatively low speeds, perhaps of the order of 50 knots.

Two separate trends have developed to change this outlook. First, as we have just noted, the foremost developers of full peripheral ACV's or Hovercraft are finding it profitable to accept much more severe hydrodynamic drag, in the interest of reducing the air gap area S_g, than would have been guessed by most experts a few years ago. Secondly, more recent research on sidewall ACV's (especially under the U. S. Navy's Captured Air Bubble Research Program) has produced greatly improved understanding of these sidewall craft. The sidewall GEM, or CAB now appears to be a very strong contender for future maritime Surface Effect Ship (SES) or ACV ship applications.

For the full-peripheral ACV or Hovercraft (at its current stage of development, with "moderate" cushion pressures), the most essential thing to be understood was the tradeoff between cushion power and propulsion power. For the CAB, the most essential thing to be understood is the tradeoff between the wavemaking propulsion power and the remainder of the propulsion power.

Previously we dealt with the ideal total specific propulsive power from Equation [26] only.

$$\frac{P_{p,i}}{W\,V_o} = \frac{D_o}{W} = \frac{1}{0.0012}\,C_{D_o}\left(\frac{1}{17.2}\,\frac{V_k}{\sqrt{w}}\right)^2 \qquad [37]$$

We must now define the ideal propulsive power to include "wavemaking" drag from Equation [2] as well.

When we seek to represent the CAB on a graph like Figure 10, we find the problem slightly complicated by the addition of the two new variables w/ℓ and Froude number $V/\sqrt{g\ell}$ or speed/length ratio $V_k/\sqrt{\ell}$. However, one of these is eliminated by relating the speed-length ratio, $V_k/\sqrt{\ell}$, to our previous speed parameter, $V_k/\sqrt{w}$:

$$\frac{V_k}{\sqrt{\ell}} = \frac{V_k}{\sqrt{w}} \sqrt{\frac{w}{\ell}} \qquad [38]$$

so only the single new variable w/ℓ need appear on the graph.

Such a graph is presented in Figure 12, showing, for simplicity, only single representative values of the variables C_{D_o} and $\left(K_{c,i}\ S_g/S\right)$.

Figure 12 displays straight lines of slopes -1 and +2, just like Figure 10; but now, the intersection between these lines is faired by a more complicated curve of total ideal specific power, strongly influenced by the wavemaking drag "hump."

In fact, we now find <u>two</u> minima in the "total" curve, when the cushion is heavily loaded, the higher-speed one being the one which we choose to call the optimum performance point. (In practice, the air gap ratio S_g/S might be reduced as the speed is reduced to such an extent that the lower minimum disappears, and the specific power improves continuously with speed reduction, at speeds below "hump speed." In fact, the cushion power has usually been neglected entirely from the optimization studies for CAB's, except to add on a 5 percent or 10 percent power margin at the end.)

One sees, in the example of Figure 12, that an increase in the specific loading parameter w/ℓ has a very slightly unfavorable effect on the value of the minimum specific power, at the higher speeds. On the other hand, an increase in w/ℓ has a noticeably favorable effect on the (dimensional) optimum speed. For example, design point B has twice the speed of design point A. On the other hand, at very high loadings (such as design B), the severe wavemaking drag hump complicates the design of the propulsion system.

Keep in mind that Figure 12 gives only one example of C_{D_o} and $K_{c,i}S_g/S$. It is easy to see that the picture can change considerably with changes in these variables.

The alert reader will now ask, Wherein has our treatment of CAB's, as reflected in Figure 12, and our preliminary treatment of full-peripheral GEM's or Hovercraft, as reflected in Figure 10, revealed any fundamental differences between the two types of craft? We have no answer, except to admit that we have found no fundamental differences at all! In treating the CAB, we have been compelled to bring in the concept of wavemaking drag, because

1. We expect such small values of cushion specific power that the component of propulsion specific power associated with wavemaking drag becomes significant by comparison, and

2. We expect somewhat higher values of the parameter w/ℓ, for the CAB, which makes the wavemaking drag larger in absolute magnitude.

However, these are differences of degree, not differences of kind. The fact is that we might just as well have introduced wavemaking drag into Figure 10 (had we not been striving for simplicity); and the fact is that Figure 12 is every bit as valid for a full-peripheral ACV or Hovercraft (with $K_{c,i}\ S_g/S = 0.002$, $C_{D_o} = 0.5$ and a rectangular cushion of $\ell/b = 2$) as it is for a CAB. Of course, such a small value for the air gap area ratio is not at all representative of current full-peripheral GEM's, but the trend of development seems to point somewhat in that direction.

Note that, since the cushion power is such a small fraction of the CAB's total power, there is little or nothing to be gained from sophistication in the method of delivering air to the cushion. Designers will probably choose to let the air be delivered directly from the compressors to the cushion, as in the full-peripheral plenum craft.

Also, it is apparent that the plenum walls at the bow and stern will preferably be compliant with the uneven surface (waves) over which the craft travels. Among the various solutions which have been proposed are:

1. To spring-suspend the bow and stern plenum walls mechanically in such a way that they will plane on the wave surfaces, as skis, at a favorable angle of attack for minimum drag.

2. To use flexible-fabric bow and stern plenum walls arranged to yield freely to wave impacts; in other words, to fit the CAB with flexible trunks or skirts at very low daylight clearances.

Before completing the discussion of ideal specific power, it would be well to return to Figure 12, to examine design points A and B again as a design exercise. The specific loading of B is four times that of point A. For example, for a given size craft, B is loaded to a gross weight of four times that of A. This is obviously advantageous from the point of view of attaining a lower structure/gross weight ratio for B and hence a higher payload/gross weight ratio. The importance of this design direction could be impressive. Further, the dimensional speed (in knots, for example) of design point B is twice that of point A; again, a very favorable factor. There is, however, an increase in specific power from about 0.06 for A to about 0.07 for B, a 16 to 17 percent increase. However, a common over-all vehicle productivity figure of merit, used in comparing vehicles of different speeds is $\frac{W V^2}{P_i}$. For example, the von Karman-Gabrielli line (to be discussed again) has only one value of this parameter, regardless of the (speed) point chosen on it. Considering point A to have a value of this productivity figure of merit of unity, B then has a value of 1.7.

Thus it could be extremely important to follow a design trend from A to B on Figure 12. What stands out as a difficulty in this design trend direction is the ever increasing drag at "hump" speed, and decreased propulsor efficiencies at the hump speed.

PROPULSOR EFFICIENCY

Figure 13 shows schematically fluid flow through an open propeller across which there is a pressure rise. Bernoulli's equation can be applied to the flow on each side of the propeller, but not across it. The ideal propulsive efficiency is the ratio of useful-power/total-power, and the useful power is thrust times velocity. From these definitions and a consideration of simple fluid momentum and energy relations, it is

possible to arrive at the ideal propulsive efficiency as a function of the thrust coefficient C_T , as shown in Figure 13.

Figure 14 contains experimental efficiency data on variable-pitch air propellers as a function of thrust coefficient C_T . By changing the constant in the ideal propulsive efficiency equation shown in Figure 13 from 2 to 1.7, a reasonable fit can be made to the upper envelope of the experimental data of Figure 14. Thus a practical air propeller efficiency is given by

$$\eta = \frac{1.7}{1 + \sqrt{1 + C_T}} \qquad [39]$$

This is a practical efficiency of 85 percent of the ideal efficiency. The ideal efficiency applies to a propeller in any fluid (water, as well as air); but the above practical efficiency applies only to a variable-pitch air propeller, pitched optimally for each value of thrust coefficient C_T .

Figure 15 shows an array of 15 air propellers (case B) on a 3,600-ton CAB vehicle of pressure/length (or specific loading/length) ratio of 0.8, having a propeller/base area ratio (S_p/S) of 0.2. Case A involves four propellers and an S_g/S ratio of 0.05. A third case, C (which is obviously impractical), involves 60 propellers and an air propeller area of 80 percent of the vehicle base area.

Using Equation [39], vehicle gross-weight/shaft-horsepower ratio is plotted for these three cases. The shaft horsepower is the variable in this plot and it involves the thrust effective power divided by the propulsive efficiency.

For Sea State 2 conditions, the weight-to-power advantage of Case C over Case A is about 35 to 40 percent at 100 knots. In case A, 50 pounds of vehicle gross weight could be had for each horsepower; in Case C, 67 to 70 pounds per horsepower could be had.

However, consider operation in Sea State 6. In this sea state, it would be desirable to maintain a speed of perhaps 50 knots; that is, a

speed somewhat higher than hump speed (35 to 40 knots). For Case A, 40 pounds per horsepower would be achieved; for Case C, 80 pounds per horsepower would be possible. This is a 100-percent advantage for Case C over Case A. In other words, twice the installed power would be required for Case A as would be needed for Case C. The cruise speed of Case C in Sea State 2 would then be 90 knots (for 80 pounds per horsepower).

Thus, the design condition that determines the size of the powerplant is not the high-speed low-sea-state condition, but rather the high-sea-state near-hump-speed condition.

Of course, Case C is not realistic for air propellers. But the same ideal propulsive efficiency could be realized using two water propulsors approximately five feet in diameter; that is, the mass flow rate for the sixty 25-foot-diameter air propellers (Case C) would be matched by two five-foot-diameter water propulsors. Figure 15 shows two scaled discs of this size at the bottom of the CAB sidewalls. The exact nature of the best future high-speed water propulsor system is, of course, not known at this time; but it would appear that one likely contender as an efficient high-speed water propulsor system would be a water-jet encased in each sidewall with an inlet-diffuser that lets the pump be subcavitating and thus highly efficient. If the sidewall encasement could avoid low inlet losses, avoid ducts with multiple right angle bends (achieve relatively straight-through flow), and avoid long ducts (and high water weights per unit diameter), a high-efficiency propulsor system could possibly result. A second high-speed water propulsor contender would appear to be supercavitating water propellers.

Calculational designs are presented in Figure 16 for both CAB's and Hovercraft, using air propellers having a propeller/base area ratio, S_p/S, of 0.2 and a size range from 100 to 10,000 tons. The figure also shows, for reference, ship and hydrofoil, as well as helicopter and airplane design regions, in terms of weight/power ratio (pounds per shaft horsepower). In this figure, the power is not the ideal power, but rather the shaft power (for both propulsion and cushion power). The

Karman-Gabrielli line (taken from Reference 11) is a straight line on the logarithmic plot, chosen empirically (by von Karman and Gabrielli) to mate with airplanes at the high-speed end and with ships at a $\frac{W}{SHP}$ of about 10,000 (which lies above the graph).

In the case of the full-peripheral ACV or Hovercraft, the daylight clearance was chosen to be six inches regardless of vehicle size, reflecting a design trend for these craft. This assumption and the ones made with respect to CAB calculations are not necessarily conservative assumptions. In the speed regime of 50 to 150 knots, however, the indicated performance potential of both of these aerostatic vehicles is so far superior to any of the other vehicles that the gap of difference could not possibly be closed by the nature of the input assumptions. For example, at 100 knots and 10,000 tons, more than a factor of 6 separates ships and CAB's for the calm water conditions for which Figure 16 is drawn (Reference 12).

For both the CAB and the Hovercraft, there is an attractive proximity to the Karman-Gabrielli line, particularly in larger sizes. The CAB shows a performance advantage in the 100-ton case relative to Hovercraft, but this advantage closes in larger sizes, because of the decreased S_g/S ratio of the Hovercraft in large sizes.

The Navy choice between these craft will likely be based on other characteristics than just those shown in Figure 16. For example, the skirted Hovercraft has an over-the-beach capability that will probably make it attractive in ship-to-shore operations. On the other hand, there appears to be an efficient sub-hump speed performance (but relatively high Froude numbers by ship standards) of CAB's that could make them attractive in a mission in which it is valuable to extend on-station time and range by slowing to sub-hump speeds.

Additionally, since CAB craft are not amphibious, and already have paid the penalties of sidewalls in the water, they probably enjoy a unique advantage in the possible use of future high-speed water propulsor systems.

For extremely long ranges (across the ocean and return without refueling, for example), nuclear power would appear to be a necessity.

The right vertical scale of Figure 16 shows nuclear propulsion (N.P.) machinery specific weight. This scale is based on 40 percent of the vehicle gross weight being available for N.P. machinery. For a 35-percent structure and outfit weight (as one example), this would provide a 25-percent payload fraction.

For these conditions, the N.P. machinery specific weights required appear to range from 20 to 60 pounds per horsepower. At least, this is a simpler condition to fulfill than the four to five pounds per horsepower required for the aircraft nuclear propulsion case.

Aerodynamics Laboratory
David Taylor Model Basin
Washington, D. C.
September 1966

REFERENCES

1. Ford, Allen G. Captured Air Bubble (CAB) High-Speed Over-Water Vehicle Report. Johnsville, Pa., May 1964. 31 p. incl. illus. (Naval Air Development Center. Rpt. NADC-WR-6412)
2. Chaplin, Harvey R. and Allen G. Ford. Some Design Principles of Ground Effect Machines. Sec. A: Introductory Survey. Wash., Apr 1966. 28 p. incl. illus. (David Taylor Model Basin. Rpt. 2121A. Aero Rpt. 1100A)(DDC AD 635 512)
3. Chaplin, Harvey R. and Allen G. Ford. Some Design Principles of Ground Effect Machines. Sec. B: Air Cushion Mechanics. Wash., Apr 1966. 34 p. incl. illus. (David Taylor Model Basin. Rpt. 2121B. Aero Rpt. 1100B)(DDC AD 635 468)
4. Chaplin, Harvey R. and Allen G. Ford. Some Design Principles of Ground Effect Machines. Sec. C: Internal Aerodynamics. Wash., Apr 1966. 28 p. incl. illus. (David Taylor Model Basin. Rpt. 2121C. Aero Rpt. 1100C) (DDC AD 636 099)
5. Chaplin, Harvey R. and Allen G. Ford. Some Design Principles of Ground Effect Machines. Sec. D: Drag. Wash., Jun 1966. 26 p. incl. illus. (David Taylor Model Basin. Rpt. 2121D. Aero Rpt. 1100D) (DDC AD 636 277)
6. Newman, J. N. and F.A.P. Poole. Wave Resistance of a Moving Pressure Distribution in a Canal. Wash., Mar 1962. 7 p. incl. illus. (David Taylor Model Basin. Rpt. 1619) (Reprinted from Schiffstechnik (Hamburg), vol. 9, Jan 1962)
7. Crewe, P. R. and W. J. Eggington. The Hovercraft; A New Concept in Maritime Transport. Royal Institution of Naval Architects. Quarterly Transaction (London), vol. 102, Jul 1960, p. 332
8. Weinblum, Georg P., Janet J. Kendrick and M. Allison Todd. Investigation of Wave Effects Produced by a Thin Body; TMB Model 4125. Wash., Nov 1952. 19 p. incl. illus. (David Taylor Model Basin. Rpt. 840)
9. Hughes, G. Frictional Resistance of Smooth Plane Surfaces in Turbulent Flow. Royal Institution of Naval Architects Quarterly Transactions (London), v. 94, 1952, p. 306

10. Republic Aviation Div. (Fairchild-Hiller Corp.) VA-3 Air Cushion Vehicle Test Program. Farmingdale, N. Y., Oct 1964. iv. illus. (RAC 2612. Contract Nonr 4500(00)

11. Gabrielli, G. and T. Von Karman. What Price Speed? Specific Power Required for Propulsion of Vehicles. Mechanical Engineering (London), v. 72, Oct 1950, p. 775-781

12. Todd, Frederick H., Harvey R. Chaplin, W. M. Ellsworth, Jr., Jacques B. Hadler & Basil V. Nakonechny. A Study of the Technical Feasibility of Future High-Speed Navy Vehicles (U). Wash., Jul 1965. [112] p. incl. illus. (David Taylor Model Basin. Rpt. C-2050) CONFIDENTIAL

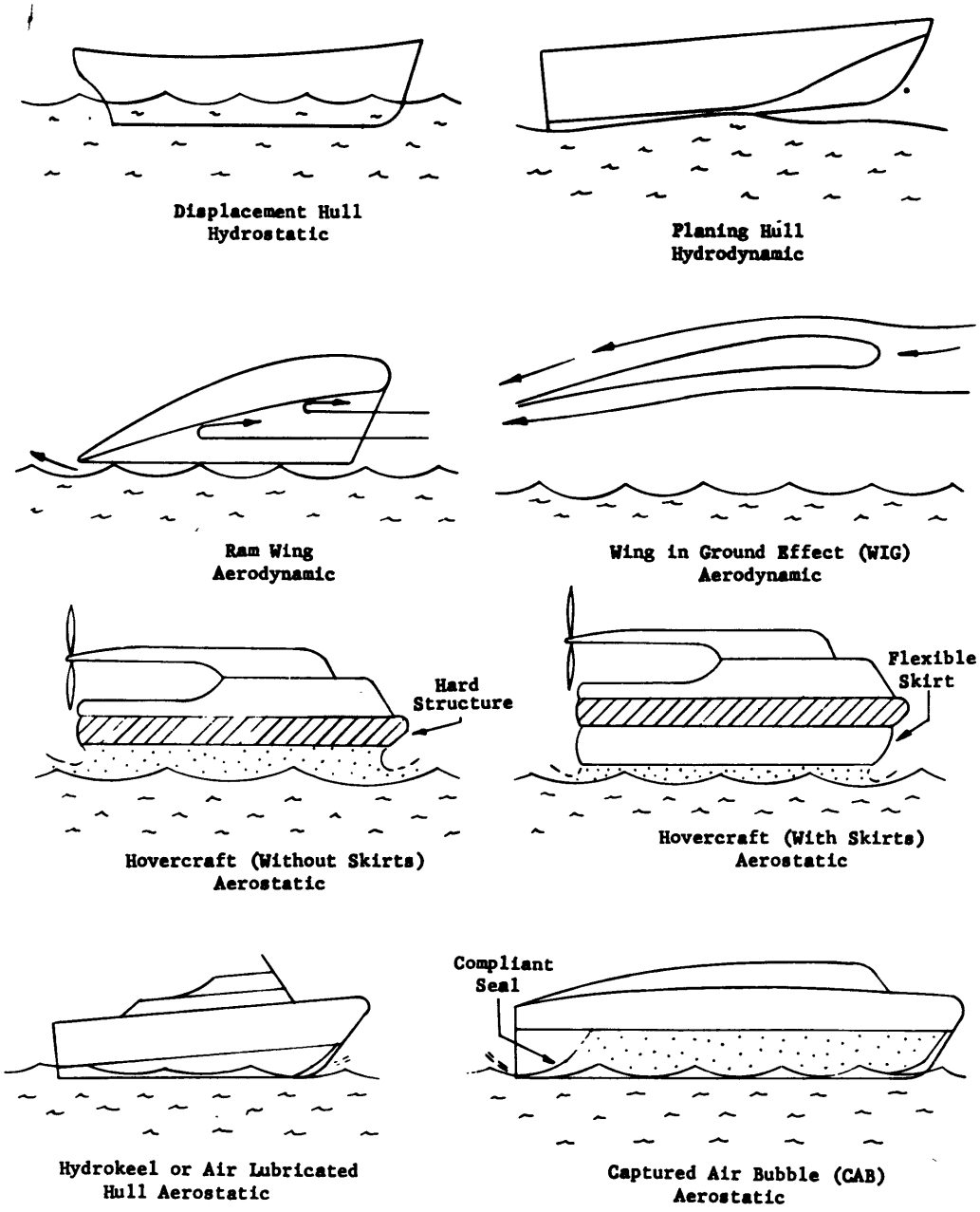

Figure 1 - Various Classes of Over-Water Vehicles With Their Principal Means of Support

Figure 2 - CAB XR-1 Experimental Research Craft at a Speed of 30 Knots

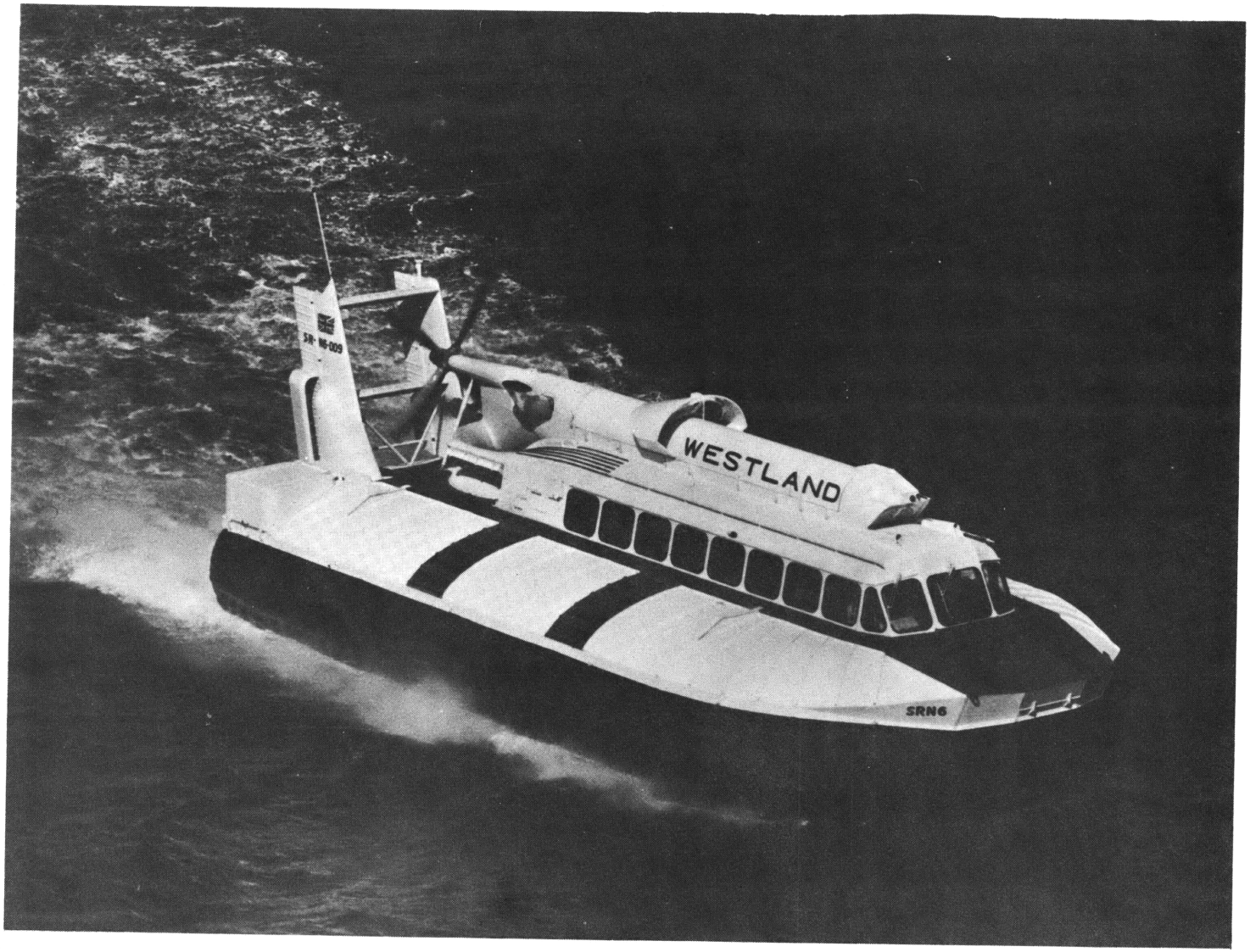

Figure 3 - Westland 10-Ton SRN-6 Hovercraft

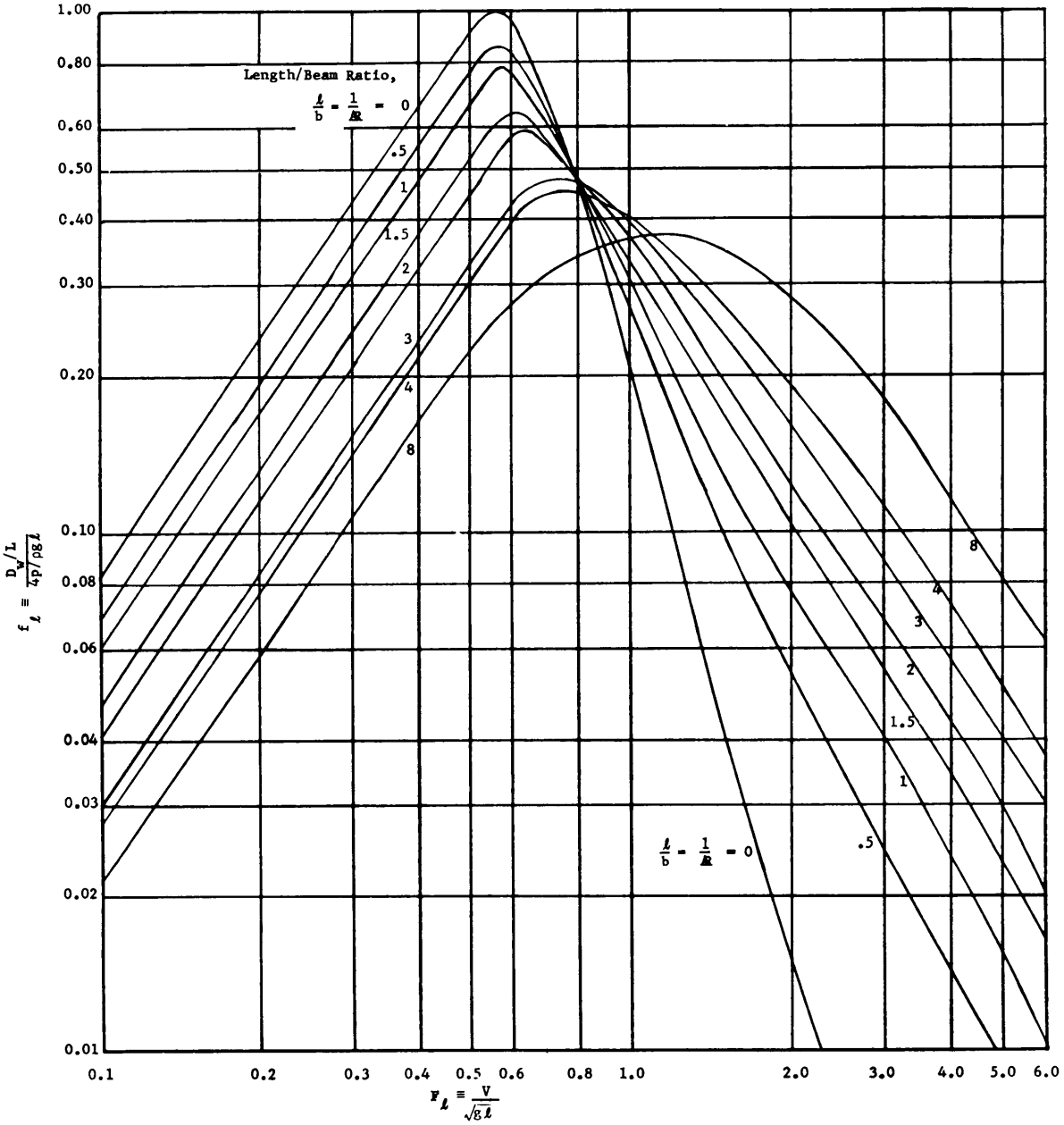

Figure 4 - Wave Drag Results, Based on Pressure Region Length ℓ, for Rectangular Pressure Planforms

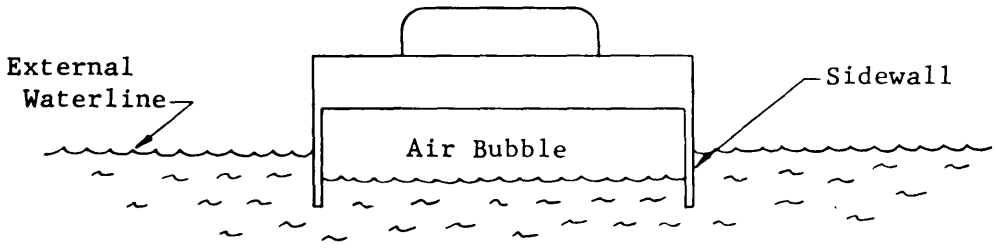

Sectional View

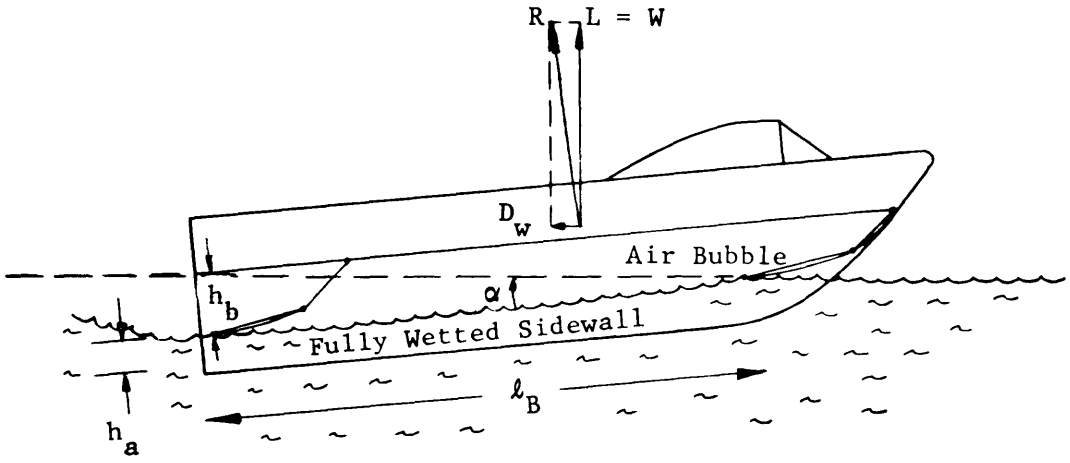

Side View

Figure 5 - Sidewall CAB ACV Showing Sidewall Wetted Areas

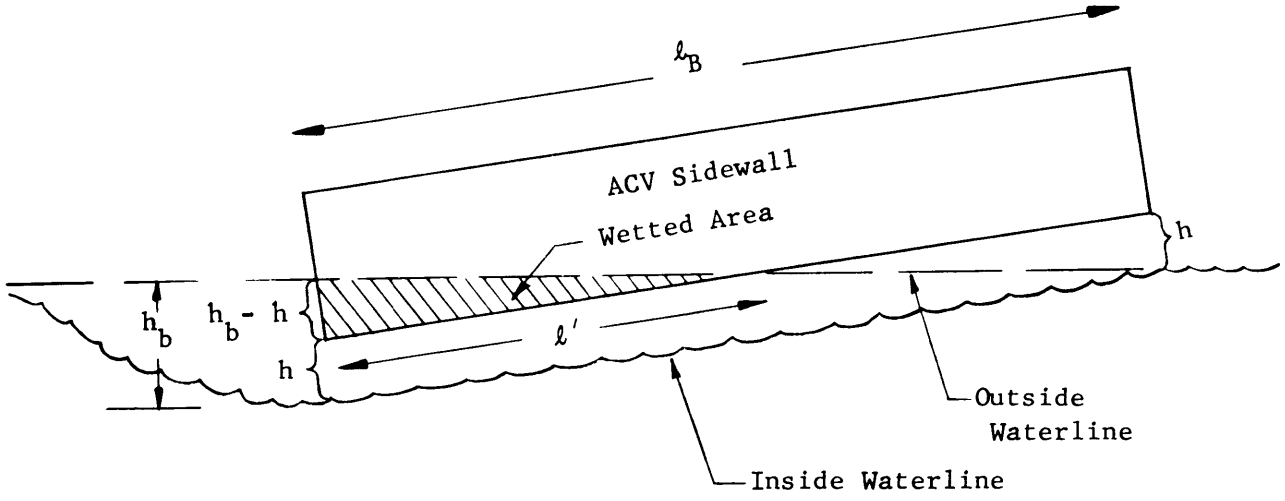

Figure 6 - Sidewall ACV With Daylight Clearance, but With Some Wetted Area

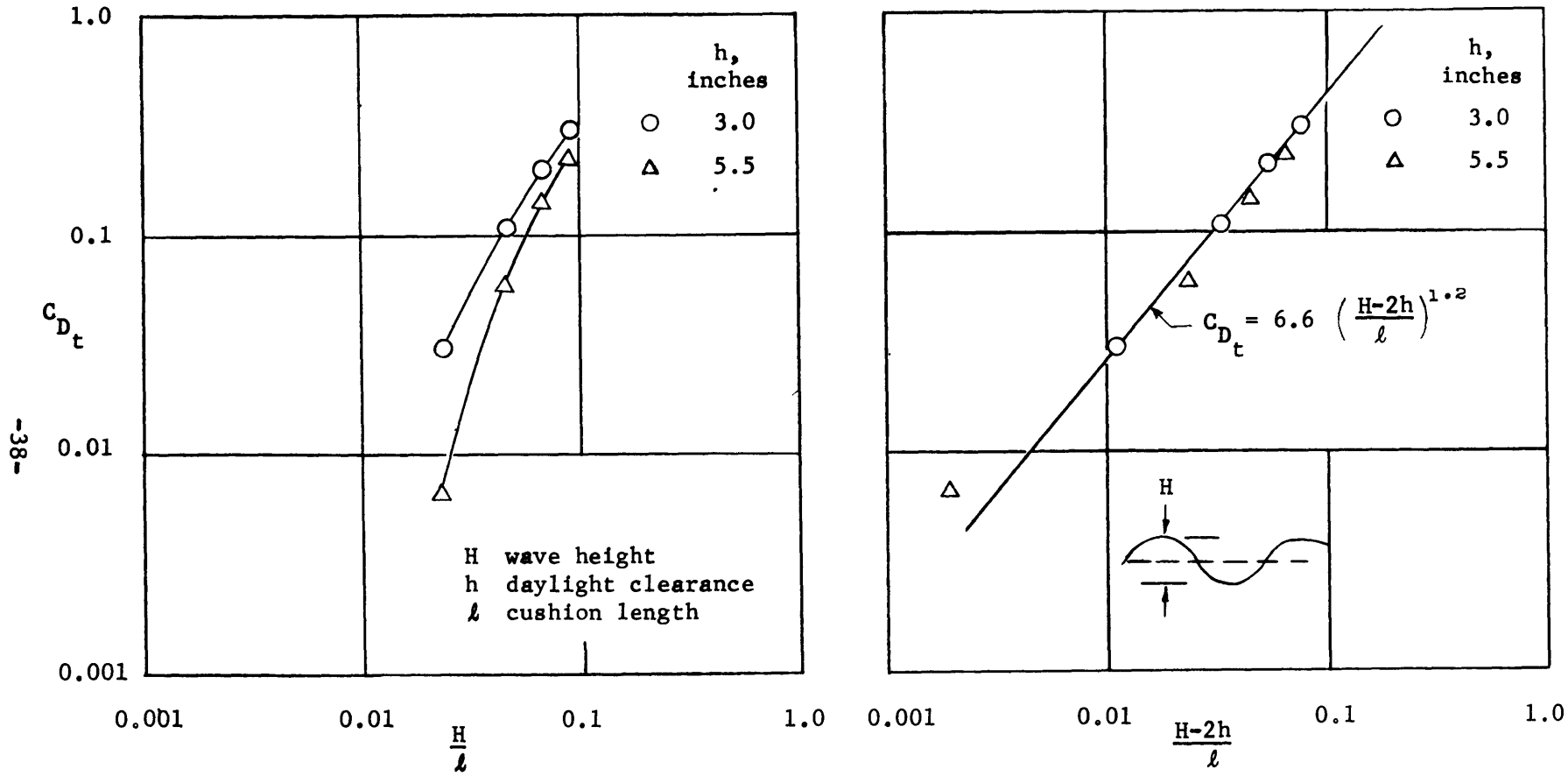

Figure 7 - Skirt or Trunk Drag Coefficient (VA-3 Data)

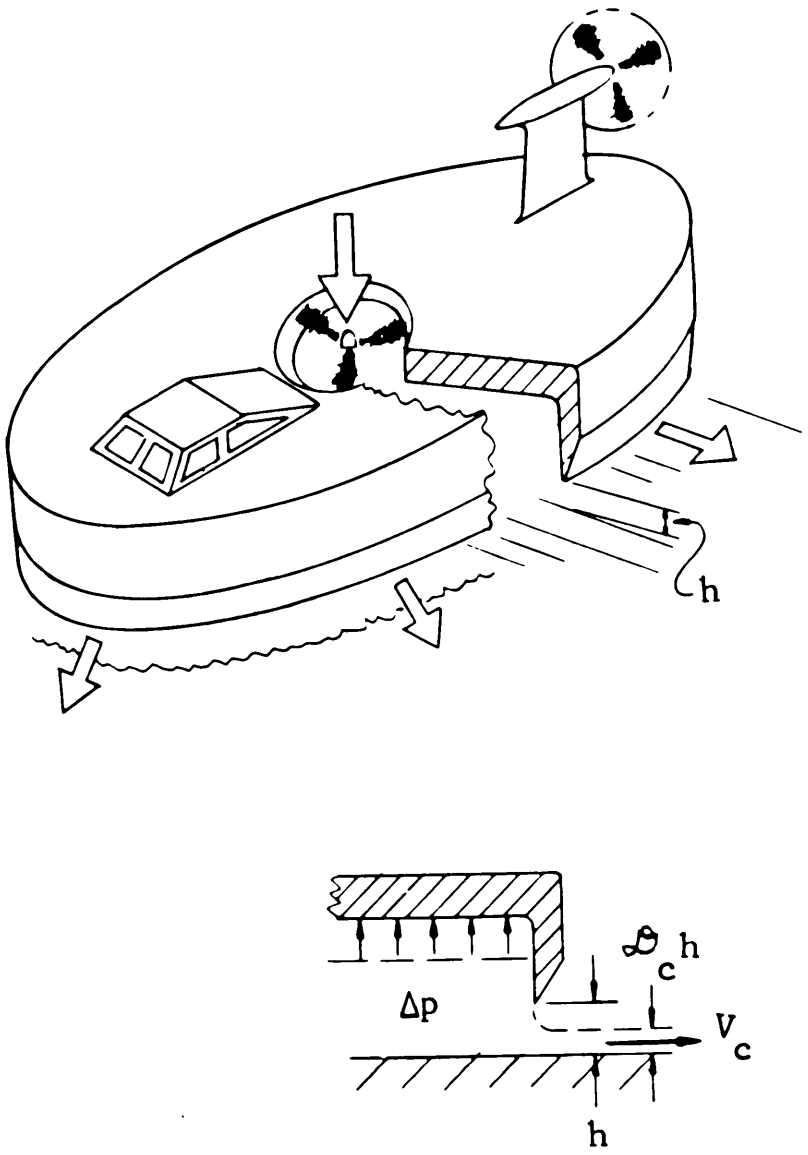

Figure 8 - Simple Plenum ACV

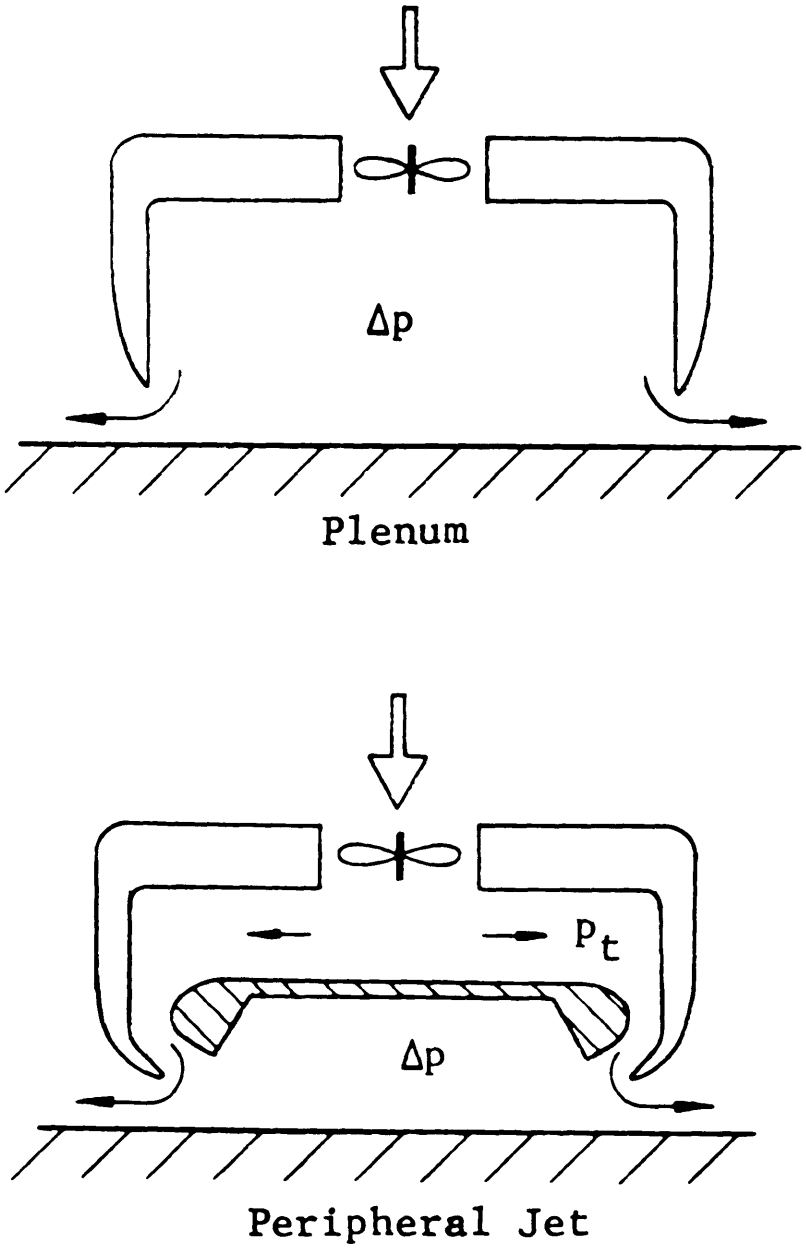

Figure 9 - Simple Plenum and Peripheral Jet Contrasted

Definitions and Expected Ranges

Plenum:

$$K_{c,i} \equiv \mathcal{O}_c \quad , \quad 0.5 < K_{c,i} < 1.0$$

Peripheral Jet:

$$K_{c,i} \equiv \mathcal{O}_c \div \Delta p/p_t \quad , \quad 0.4 < K_{c,i} < 1.0$$

$$[W \doteq \Delta p \; S \; ; \quad \rho_a = 0.00238 \text{ slugs/ft}^3]$$

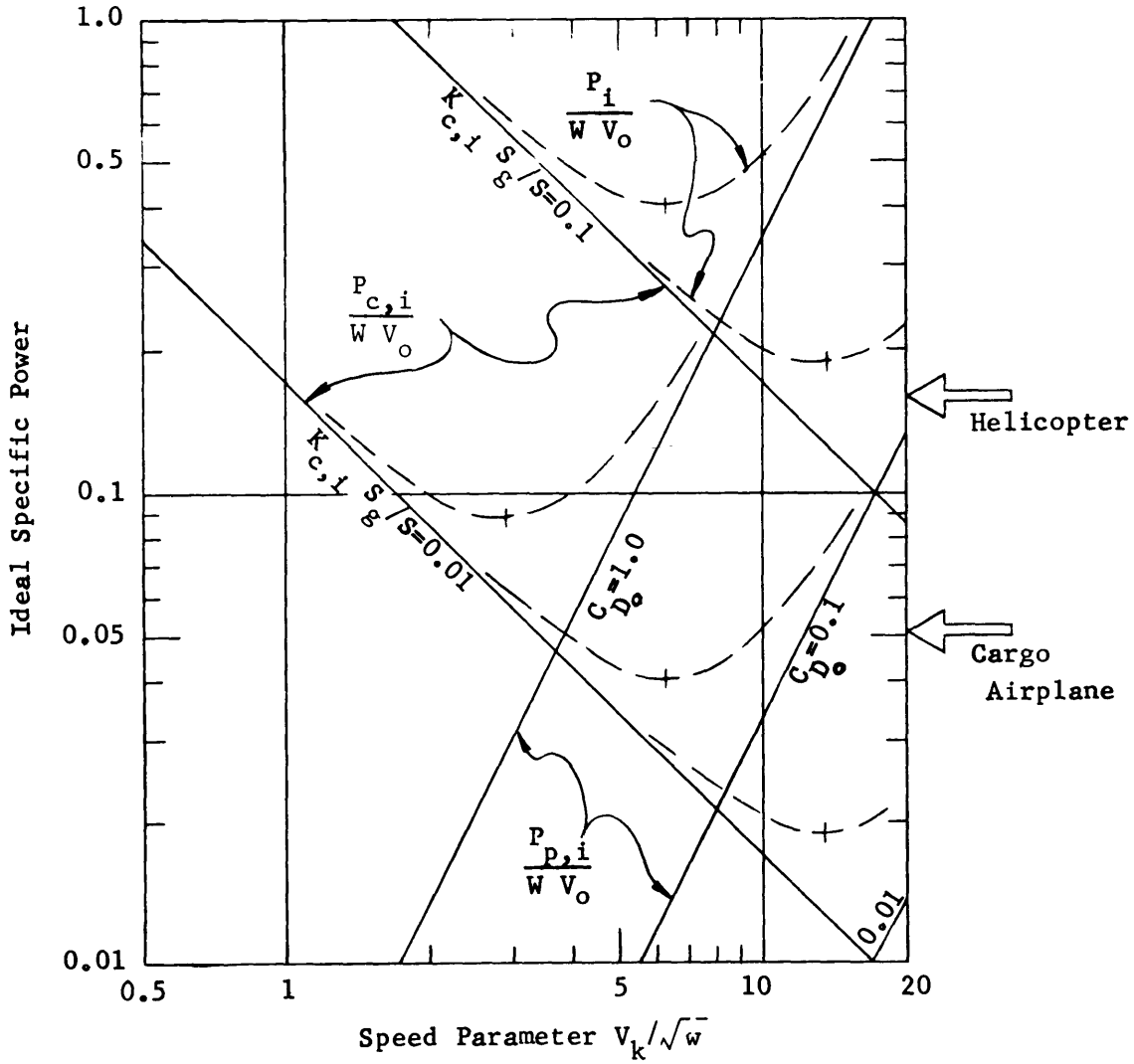

Figure 10 - Ideal Specific Power Versus Speed Parameter as Function of Gap Area Ratio and Total Drag Coefficient (Effect of forward speed on cushion power is neglected.)

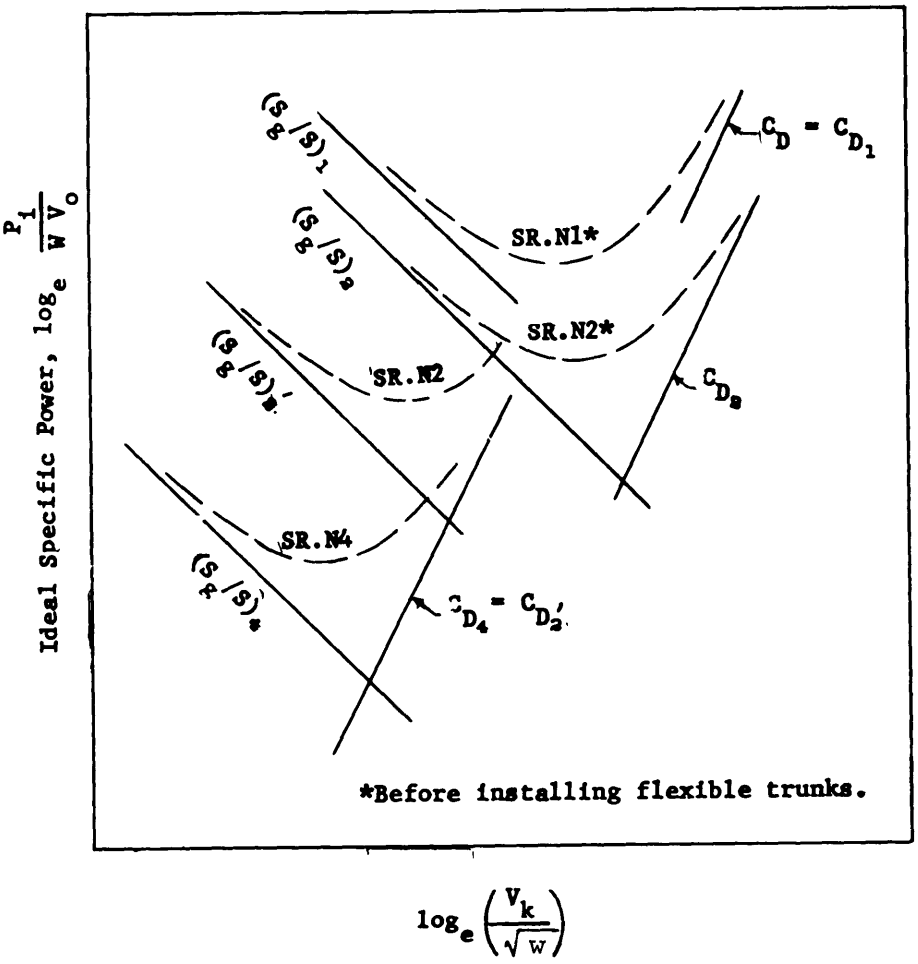

Note: Compare with Figure 10

Figure 11 - Ideal Specific Power Versus Speed Parameter
Qualitative Comparison to Existing Hovercraft

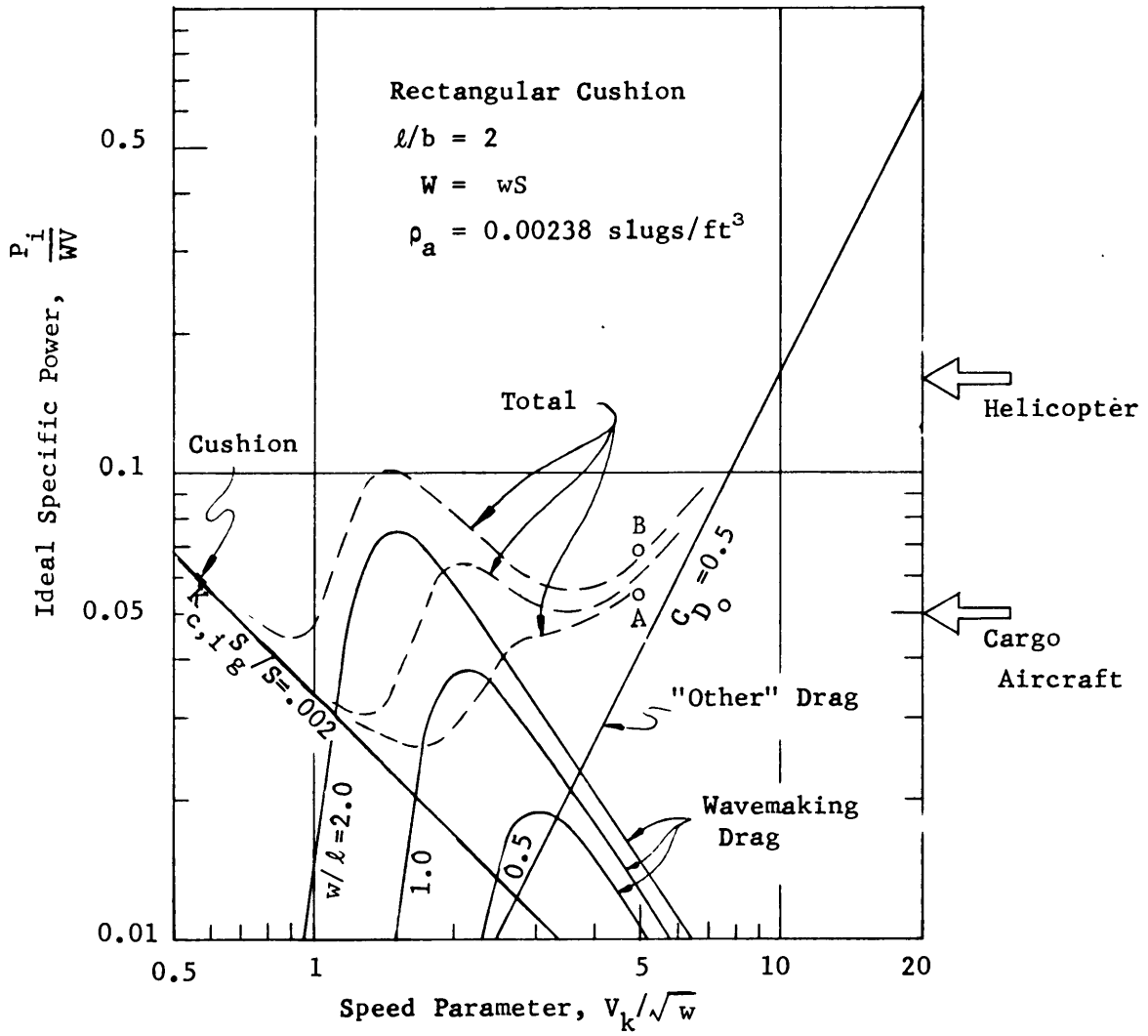

Figure 12 - Ideal Specific Power Versus Speed Parameter for a CAB Craft With Various Cushion Loadings, w/ℓ

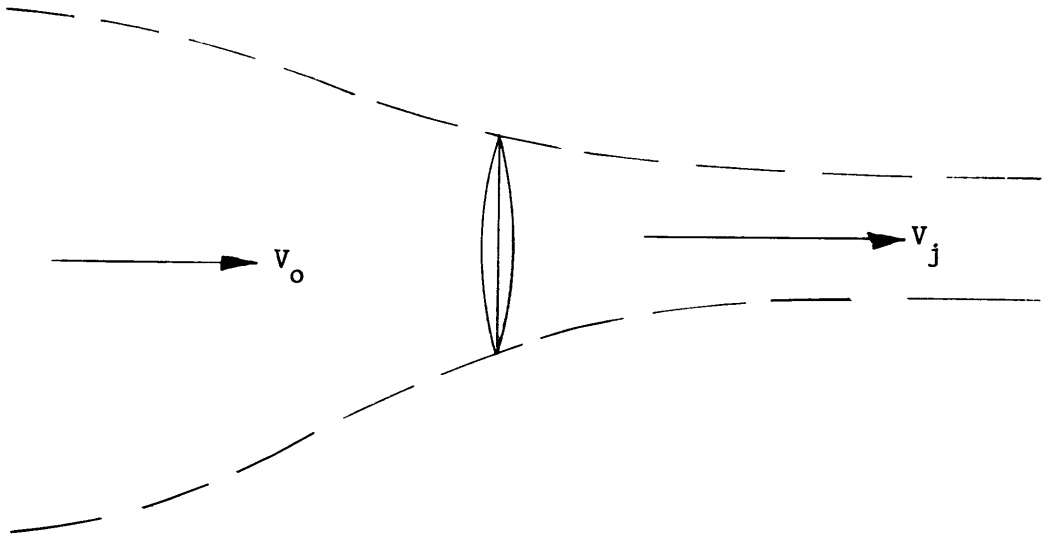

Ideal Propulsive Efficiency

$$T = \dot{m}\left(V_j - V_o\right)$$

$$P = \frac{1}{2}\dot{m}\left(V_j^2 - V_o^2\right)$$

$$\eta_I = \frac{2}{1 + \sqrt{1 + C_T}}$$

where

$$C_T = \frac{T}{\frac{1}{2}\rho V_o^2 S_p}$$

Figure 13 - Ideal Propulsive Efficiency Derived From Momentum and Energy Relations

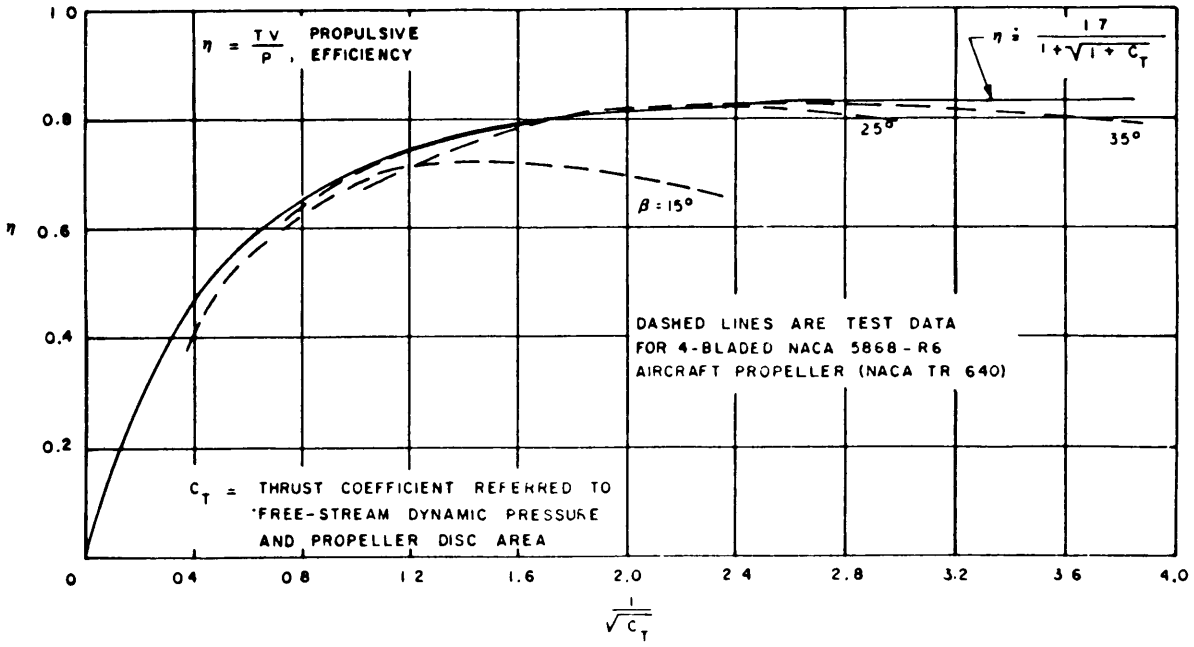

Figure 14 - Air Propeller Efficiency

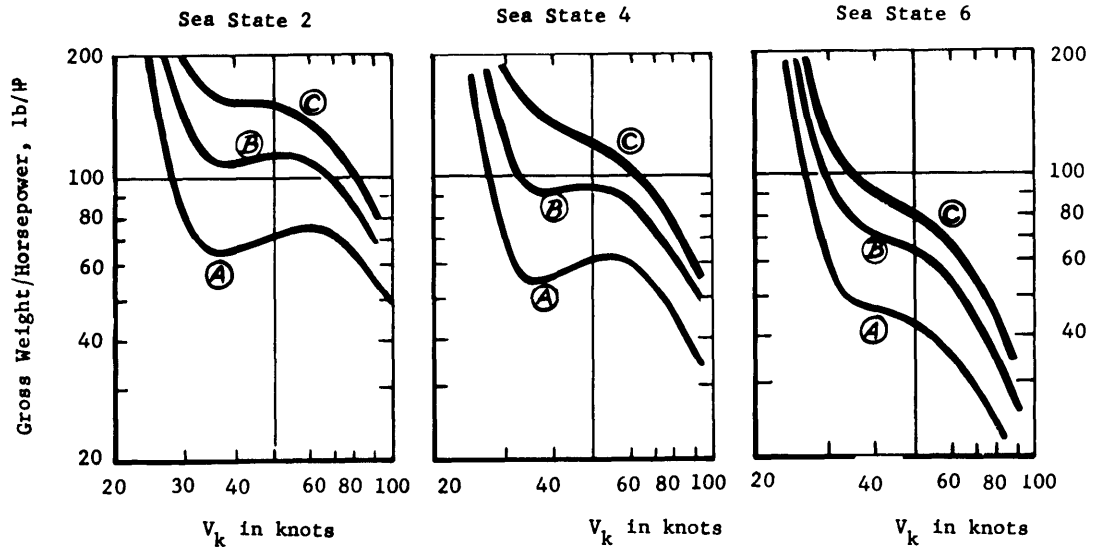

Figure 15 - Air Propeller Efficiency as a Function of Propeller/Base Area Ratio and Sea State for a Large CAB

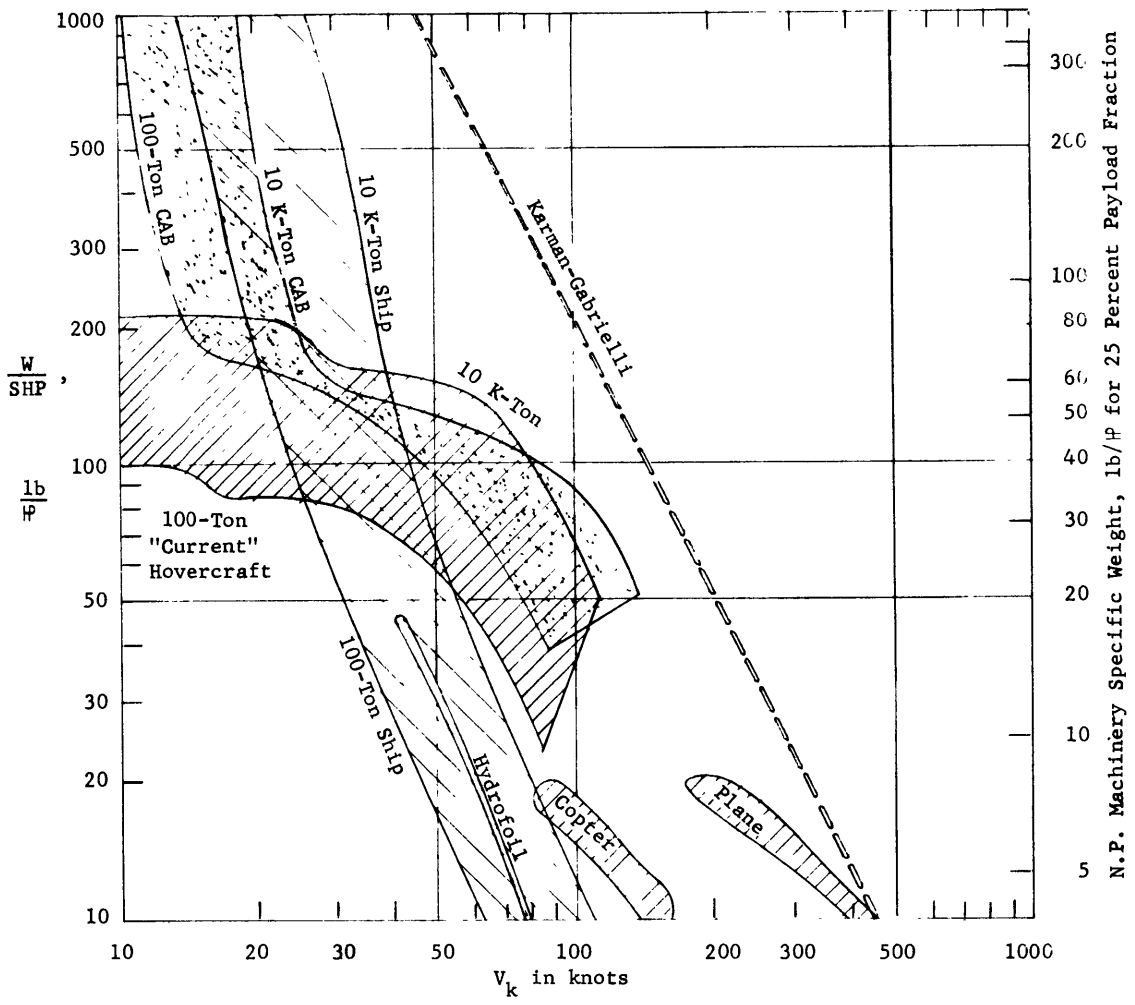

Figure 16 - Comparison of Different Over-Water Types of Vehicle

DISTRIBUTION LIST

Copies	
1	NAVAIR(530C)
4	NAVAIR(604)
20	DDC
1	CDR, NATC (Dir, TPS)
1	CO, NADC
5	Scientific & Tech. Info, Facility Bethesda, Md. (Attn: NASA Rep. (S-AK/DL)
2	ONR (461)
1	DIR, NRL (2027)
1	Supt., Naval Post-graduate Sch. Monterey, Calif.
3	CHBUSHIPS (335)
1	CHBUSHIPS (421)
1	Commandant, U.S. Marine Corps (A04E) C-4 Div.
1	CNO (Op 07T6)
1	CNO (Op 0725)
1	CO, Office of Naval Res. Br. Office, London Navy 100, Box 39, FPO New York City, N.Y.
1	DIR, Langley Res. Center (Attn: Tech. Lib.)
1	Chief of Transportation (TCDRD), Army
1	Chief of Transportation (TCDTE), Army
1	CO, U.S. Army Transportation Research Command Fort Eustis, Virginia
1	Chief of Research and Development Department of the Army (Attn: Res. Support Div.)
1	Chief, European Res. Office U.S. Army R&D Liaison Grp., APO 757 New York City, N.Y. (Attn: TC Liaison Officer)
1	Aerophysics Co., Wash., D.C.
1	Aerospace Corp. Los Angles , Calif. (Attn: Library Tech. Doc. Grp.)
1	Air Vehicle Corp. San Diego, Calif.
1	Allis-Chalmers Mfg. Co. Milwaukee, Wisc.
1	American Mach, & Foundry Co. Mechanics Research Div. Niles, Illinois
1	Avco Corp. New York, N.Y.
1	Beech Aircraft Corp. Wichita, Kansas
1	Bell Aerosystems Co. Buffalo, N.Y. (Attn: Chief Librarian)

DISTRIBUTION LIST

Copies	
1	Bell Helicopter Co. Fort Worth, Texas
1	Bertelsen Mfg. Co. Neponset, Ill.
1	Boeing Company Wichita, Kansas (Attn: Chief Engr.)
1	Boeing Company Transport Division Seattle, Wash. (Attn: Lib.)
1	Boeing Company Vertol Division Morton, Pa.
1	Booz-Allen Applied Research, Inc. Bethesda, Md.
1	Borg-Warner Corp. Ingersoll Kalamazoo Div. Kalamazoo, Mich.
1	Cessna Aircraft Co. Research Dept. Wichita, Kansas
1	Chrysler Corp. Defense Operations Div. Detroit, Mich. (Attn: Lib.)
1	Cornell Aeronautical Lab., Inc. Buffalo 21, New York
1	Cornell-Guggenheim Aviation Safety Center New York, N.Y. (Attn: Director)
1	Curtiss-Wright Corp. Wash., D.C.
1	Curtiss-Wright Corp. Wright Aeronautical Div. Wood-Ridge, N.J. (Attn: Tech. Lib.)
1	Douglas Aircraft Co., Inc. El Segundo, Calif.
1	Fairchild Stratos Corp. Fairchild Acft. & Missiles Div. Hagerstown, Md.
1	Food Machinery & Chem. Corp. San Jose, Calif.
1	The Ford Motor Co. Aeronautical Div. Newport Beach, Calif.
1	Engineering Development Corp. Englewood, Colo.
1	The Garrett Corp. Airesearch Mfg. Co. Phoenix, Arizona (Attn: Lib.)
1	General Electric Co. FPD Tech. Info. Center Cincinnati, Ohio
1	General Electric Co. Small Acft. Engine Dept. West Lynn, Mass.
1	General Dynamics Corp. Convair Fort Worth Oper. Div. Fort Worth, Texas (Attn: Lib.)
1	General Dynamics Corp. Convair Division Dept. of Aero. Engrg. San Diego, Calif.

DISTRIBUTION LIST

Copies		Copies	
1	General Dynamics Corp. Electric Boat Division Groton, Conn.	1	North American Aviation, Inc. Autonetics Div. Downey, Calif.
1	Goodyear Aircraft Corp. Akron, Ohio	1	North American Aviation, Inc. Columbus, Ohio
1	Grumman Aircraft Engr. Corp. Bethpage, L.I., N.Y.	1	Northrop Corp. Hawthorne, Calif.
1	Gyrodyne Co. of America, Inc. Dept. of Aero. Engineering St. James, L.I., N.Y.	1	Piasecki Aircraft Corp. Phil., Pa.
1	Hiller Aircraft Corp. Advanced Research Dept. Palo Alto, Calif.	1	Radio Corp. of America Missile Electronics & Controls Burlington, Mass. (Attn: Lib.)
1	Hughes Tool Co. Air-Craft Division Culver City, Calif. (Attn: Chief, Tech. Engr.)	1	Republic Aviation Corp. Farmingdale, L.I., N.Y. (Attn: Mil. Contr. Dept.)
1	Kaman Aircraft Corp. Bloomfield, Conn.	1	Ryan Aeronautical Co. San Diego, Calif. (Attn: Chief Engineer)
1	Kellett Acft. Corp. Willow Grove, Pa.	1	Solar Aircraft Co. San Diego, Calif.
1	Kettenberg Boats, Inc. San Diego, Calif.	1	Tacoma Boat Bldg. Co., Inc. Tacoma, Wash.
1	Ling-Temco Vought, Inc. Dallas, Texas	1	H.M. Tiedemann & Co., Inc. New York, N.Y.
1	Lockheed Aircraft Corp. Burbank, Calif.	1	United Aircraft Corp. Sikorsky Aircraft Div. Stratford, Conn.
1	Martin-Marietta Corp. Baltimore, Md. (Attn: Library & Doc. Sec.)	1	United Aircraft Corp. Research Dept. East Hartford, Conn.
1	McDonnell Aircraft Corp. St. Louis, Missouri	1	Vehicle Research Corp. Pasadena, Calif.

DISTRIBUTION LIST

Copies		Copies	
1	Martin-Marietta Corp. Orlando Div. Orlando, Fla.	1	Rensselaer Polytechnic Inst. Dept. of Aero. Engrg. Troy, New York
1	Univ. of Calif. Inst. of Engrg. Res. Berkeley, Calif.	1	Univ. of Southern Calif. Engrg. Center Los Angeles, Calif.
1	Univ. of Calif. Dept. of Engineering Los Angeles, Calif.	1	Stevens Institute of Tech. Hoboken, N.J.
1	Catholic Univ. Dept. of Mech. and Aero. Engrg. Wash., D.C.	1	Virginia Poly. Inst. Carol M. Newman Library Blacksburg, Va.
1	Johns Hopkins Univ. Dept. of Aeronautics Baltimore, Md.	1	Univ. of Wichita Dept. of Engrg. Wichita, Kan.
1	Univ. of Louisville Speed Scientific Sch. Lib. Louisville, Ky.	1	Air War College, Air Univ. Maxwell AFB, Alabama (Attn: Evaluation Staff)
1	MIT, Hayden Library Ser. & Documents Div. Cambridge, Mass.	1	Hdqs., U.S. Air Force (AFRDT-EX) Deputy Chief of Staff Research & Technology Wash., D.C.
1	Iowa State University Iowa Inst. for Hydraulic Res. Iowa City, I.	1	Executive Director Air Force Office of Scientific Research (SRIL) Dept. of the Air Force Wash., D.C.
1	Univ. of Minn. Rosemount Aeronautical Labs. Dept. of Engrg. Minneapolis, Minn.	1	Chief, Office of Research and Development Maritime Adm. Wash., D.C.
1	Miss. State College Aerophysics Dept. State College, Miss.	1	MEL
1	Princeton Univ. Forrestal Res. Center Princeton, N.J. (Attn: Libr.)	1	NAEC
		1	IDA
		1	CNA
		1	CNO (Op 723)

Unclassified

Security Classification

DOCUMENT CONTROL DATA - R&D

(Security classification of title, body of abstract and indexing annotation must be entered when the overall report is classified)

1 ORIGINATING ACTIVITY (Corporate author)	2a REPORT SECURITY CLASSIFICATION
Aerodynamics Laboratory David Taylor Model Basin Washington, D. C. 20007	Unclassified
	2b GROUP

3 REPORT TITLE

PROGRESS IN AIR CUSHION VEHICLES

4 DESCRIPTIVE NOTES *(Type of report and inclusive dates)*

5 AUTHOR(S) *(Last name, first name, initial)*

Ford, Allen G.

6 REPORT DATE	7a TOTAL NO OF PAGES	7b NO OF REFS
October 1966	51 [vii]	12

8a CONTRACT OR GRANT NO	9a ORIGINATOR'S REPORT NUMBER(S)
b PROJECT NO. Subproject ZF 013 01 01	Report 2280
c Problem Number 060-001	9b OTHER REPORT NO(S) *(Any other numbers that may be assigned this report)*
d	Aero Report 1116

10 AVAILABILITY/LIMITATION NOTICES

The distribution of this document is unlimited.

11 SUPPLEMENTARY NOTES	12 SPONSORING MILITARY ACTIVITY
	Commander Naval Ship Systems Command Washington, D. C. 20360

13 ABSTRACT

An analysis is made of the various drag and power components applicable to the Captured Air Bubble (CAB) vehicle and to Hovercraft. These are wavemaking drag, sideboard drag, skirt (or trunk) drag, external aerodynamic drag, ram (or momentum) drag, and cushion power. Equations for the components are used to follow trends in Hovercraft and CAB development, wave drag playing an important role in the latter case. However, it is found that the equations for the two craft show no fundamental differences of kind, only differences of degree.

The subject of propulsor efficiency is then treated for the air propeller. It is shown that to achieve high efficiencies, large propeller-area/base-area ratios are required. Water propulsor systems are then suggested as a means of obviating the disc-area problem, although significant development would be required in this case.

Finally, a comparison of vehicles is made on the basis of weight/power ratio. The indicated performance potential of air cushion vehicles (ACV's), of both the Hovercraft and the CAB types. is shown to be very high compared with other vehicles in high-speed over-water operation.

DD FORM 1 JAN 64 1473

Unclassified

Security Classification

Unclassified

Security Classification

14 KEY WORDS	LINK A		LINK B		LINK C	
	ROLE	WT	ROLE	WT	ROLE	WT
Air Cushion Vehicles						
Captured Air Bubble						
Ground Effect Machines						
Drag						
External Aerodynamic Drag						
Ram Drag						
Sidewall Drag						
Trunk Drag						
Wavemaking Drag						
Cushion Power						
Total Specific Power						
Propulsor Efficiency						
Hovercraft						

INSTRUCTIONS

1. ORIGINATING ACTIVITY: Enter the name and address of the contractor, subcontractor, grantee, Department of Defense activity or other organization *(corporate author)* issuing the report.

2*a*. REPORT SECURITY CLASSIFICATION: Enter the overall security classification of the report. Indicate whether "Restricted Data" is included. Marking is to be in accordance with appropriate security regulations.

2*b*. GROUP: Automatic downgrading is specified in DoD Directive 5200.10 and Armed Forces Industrial Manual. Enter the group number. Also, when applicable, show that optional markings have been used for Group 3 and Group 4 as authorized.

3. REPORT TITLE: Enter the complete report title in all capital letters. Titles in all cases should be unclassified. If a meaningful title cannot be selected without classification, show title classification in all capitals in parenthesis immediately following the title.

4. DESCRIPTIVE NOTES: If appropriate, enter the type of report, e.g., interim, progress, summary, annual, or final. Give the inclusive dates when a specific reporting period is covered.

5. AUTHOR(S): Enter the name(s) of author(s) as shown on or in the report. Enter last name, first name, middle initial. If military, show rank and branch of service. The name of the principal author is an absolute minimum requirement.

6. REPORT DATE: Enter the date of the report as day, month, year; or month, year. If more than one date appears on the report, use date of publication.

7*a*. TOTAL NUMBER OF PAGES: The total page count should follow normal pagination procedures, i.e., enter the number of pages containing information.

7*b*. NUMBER OF REFERENCES: Enter the total number of references cited in the report.

8*a*. CONTRACT OR GRANT NUMBER: If appropriate, enter the applicable number of the contract or grant under which the report was written.

8*b*, 8*c*, & 8*d*. PROJECT NUMBER: Enter the appropriate military department identification, such as project number, subproject number, system numbers, task number, etc.

9*a*. ORIGINATOR'S REPORT NUMBER(S): Enter the official report number by which the document will be identified and controlled by the originating activity. This number must be unique to this report.

9*b*. OTHER REPORT NUMBER(S): If the report has been assigned any other report numbers *(either by the originator or by the sponsor)*, also enter this number(s).

10. AVAILABILITY/LIMITATION NOTICES: Enter any limitations on further dissemination of the report, other than those imposed by security classification, using standard statements such as:

(1) "Qualified requesters may obtain copies of this report from DDC."

(2) "Foreign announcement and dissemination of this report by DDC is not authorized."

(3) "U. S. Government agencies may obtain copies of this report directly from DDC. Other qualified DDC users shall request through _____."

(4) "U. S. military agencies may obtain copies of this report directly from DDC. Other qualified users shall request through _____."

(5) "All distribution of this report is controlled. Qualified DDC users shall request through _____."

If the report has been furnished to the Office of Technical Services, Department of Commerce, for sale to the public, indicate this fact and enter the price, if known.

11. SUPPLEMENTARY NOTES: Use for additional explanatory notes.

12. SPONSORING MILITARY ACTIVITY: Enter the name of the departmental project office or laboratory sponsoring *(paying for)* the research and development. Include address.

13 ABSTRACT: Enter an abstract giving a brief and factual summary of the document indicative of the report, even though it may also appear elsewhere in the body of the technical report. If additional space is required, a continuation sheet shall be attached.

It is highly desirable that the abstract of classified reports be unclassified. Each paragraph of the abstract shall end with an indication of the military security classification of the information in the paragraph, represented as *(TS), (S), (C), or (U)*

There is no limitation on the length of the abstract. However, the suggested length is from 150 to 225 words.

14. KEY WORDS: Key words are technically meaningful terms or short phrases that characterize a report and may be used as index entries for cataloging the report. Key words must be selected so that no security classification is required. Identifiers, such as equipment model designation, trade name, military project code name, geographic location, may be used as key words but will be followed by an indication of technical context. The assignment of links, roles, and weights is optional.

Unclassified

Security Classification